IZMIR KATIP CELEBI UNIVERSITY ★ GRADUATE SCHOOL OF SCIENCE ENGINEERING AND TECHNOLOGY

MODELLING, ANALYSIS AND EXPERIMENTAL VERIFICATION OF PNEUMATIC BRAKE SYSTEM

M.Sc. THESIS

İbrahim Can GÜLERYÜZ

Department of Mechanical Engineering

Thesis Advisor: Asst. Prof. Dr. Özgün BAŞER

JUNE 2017

IZMIR KATIP CELEBI UNIVERSITY ★ GRADUATE SCHOOL OF SCIENCE ENGINEERING AND TECHNOLOGY

MODELLING, ANALYSIS AND EXPERIMENTAL VERIFICATION OF PNEUMATIC BRAKE SYSTEM

M.Sc. THESIS

İbrahim Can GÜLERYÜZ
Y130105016

Department of Mechanical Engineering

Thesis Advisor: Asst. Prof. Dr. Özgün BAŞER

JUNE 2017

İZMİR KÂTİP ÇELEBİ ÜNİVERSİTESİ ★ FEN BİLİMLERİ ENSTİTÜSÜ

HAVALI FREN SİSTEMİNİN MODELLENMESİ, ANALİZİ VE DENEYSEL OLARAK DOĞRULANMASI

YÜKSEK LİSANS TEZİ

İbrahim Can GÜLERYÜZ
Y130105016

Makina Mühendisliği Anabilim Dalı

Tez Danışmanı: Yrd. Doç. Dr. Özgün BAŞER

HAZİRAN 2017

İbrahim Can GÜLERYÜZ, a M.Sc. student of iKCU Graduate School of Science Engineering and Technology student ID Y130105016, successfully defended the thesis entitled "MODELLING, ANALYSIS AND EXPERIMENTAL VERIFICATION OF PNEUMATIC BRAKE SYSTEM", which he prepared after fulfilling the requirements specified in the associated legislations, before the jury whose signatures are below.

Thesis Advisor : **Asst. Prof. Dr. Özgün BAŞER** .....
Izmir Katip Celebi University

Jury Members : **Asst. Prof. Dr. Ziya Haktan KARADENİZ**.....
Izmir Katip Celebi University

Prof. Dr. Zeki KIRAL .....
Dokuz Eylul University

Date of Submission : 06 June 2017
Date of Defense : 19 June 2017

To my family,

FOREWORD

I express sincere appreciation to:

Asst. Prof. Dr. Özgün BAŞER, my principal advisor, for his guidance, insight and endless patience throughout this thesis;

BMC Company's Test Department's Chief Orcan ÖZELMAS and members for their generous support during vehicle tests;

I would also like to thank my wife and my parents for all their support and encouragement throughout this journey.

June 2017

İbrahim Can GÜLERYÜZ
(Mechanical Engineer)

TABLE OF CONTENTS

Page

ABBREVIATIONS

ABS	**:** Anti-lock Braking System
ACC	**:** Adaptive Cruise Control
AEBS	**:** Advanced Emergency Braking System
CD	**:** Current Design
BC	**:** Brake Chamber
DP1	**:** Design Point 1
DP2	**:** Design Point 2
DP3	**:** Design Point 3
DP4	**:** Design Point 4
DP5	**:** Design Point 5
ESC	**:** Electronic Stability Control
FBV	**:** Foot Brake Valve
FB	**:** Foundation Brake
LDWS	**:** Lane Departure Warning System
MFDD	**:** Mean Fully Developed Deceleration
RV	**:** Relay Valve
TCS	**:** Traction Control System
TPMS	**:** Tire Pressure Monitoring System

SYMBOLS

A_{b_f} : Cross sectional area of front brake chamber diaphragm
A_{b_r} : Cross sectional area of rear brake chamber diaphragm
A_{b_rv} : Cross sectional area of relay piston
A_v : Orifice cross sectional area of FBV
A_{v_rv} : Orifice cross sectional area of relay valve
b_f : Viscous friction coefficient of front brake chamber
b_r : Viscous friction coefficient of rear brake chamber
b_{rv} : Viscous friction coefficient of relay valve
C_d : Discharge coefficient of FBV
C_{d_rv} : Discharge coefficient of relay valve
C_r : Critical pressure ratio
dP_f : Pressure drop in front circuit
dP_r : Pressure drop in rear circuit
d_{1_2} : Inner diameter of pipe 1/2"
d_8 : Inner diameter of pipe Ø8x1
d_{10} : Inner diameter of pipe Ø10x1
d_{12} : Inner diameter of pipe Ø12x1.5
F_{C_f} : Seat contact force of front brake chamber
F_{C_r} : Seat contact force of rear brake chamber
F_{C_rv} : Seat contact force of relay valve
F_{load_f} : Load force of front foundation brake
F_{load_r} : Load force of rear foundation brake
F_{pedal} : Brake pedal force
F_{PL_f} : Pre load spring force of front brake chamber
F_{PL_r} : Pre load spring force of rear brake chamber
F_{PL_rv} : Pre load spring force of relay valve
k_f : Return spring constant of front brake chamber
k_r : Return spring constant of rear brake chamber
k_{rv} : Return spring constant of relay valve
L_{1_2} : Total length of pipe 1/2"
L_8 : Total length of pipe Ø8x1
L_{10} : Total length of pipe Ø10x1
L_{12} : Total length of pipe Ø12x1.5
m_f : Push rod mass of front brake chamber
m_r : Push rod mass of rear brake chamber
m_{rv} : Relay piston mass
n : Exponent of polytropic expansion process
n_f : Number of brake chamber at front axle
n_r : Number of brake chamber at rear axle
P_{atm} : Atmospheric pressure

$\mathbf{P_f}$: Front brake chamber pressure
$\mathbf{P_{FBV}}$: Predominance pressure of FBV
$\mathbf{P_{f\_exp}}$: Experimental front brake chamber pressure
$\mathbf{P_r}$: Rear brake chamber pressure
$\mathbf{P_{r\_exp}}$: Experimental rear brake chamber pressure
$\mathbf{P_{rv}}$: Control port pressure of relay valve
$\mathbf{P_{S\_f}}$: Front supply tank pressure
$\mathbf{P_{S\_r}}$: Rear supply tank pressure
$\mathbf{P_{st}}$: Steady state system pressure
$\mathbf{P_{th\_rv}}$: Threshold pressure of relay valve
$\mathbf{P_{0\_f}}$: Initial pressure of front brake chamber
$\mathbf{P_{0\_r}}$: Initial pressure of rear brake chamber
$\mathbf{P_{0\_rv}}$: Initial control port pressure of relay valve
$\mathbf{\dot{P}_f}$: Pressure rate of front brake chamber
$\mathbf{\dot{P}_r}$: Pressure rate of rear brake chamber
$\mathbf{\dot{P}_{rv}}$: Pressure rate of control chamber
$\mathbf{R}$: Gas constant
$\mathbf{T}$: Air temperature
$\mathbf{t_{delay}}$: Actuating/delay time
$\mathbf{t_f}$: Elapsed time for front brake chamber
$\mathbf{t_r}$: Elapsed time for rear brake chamber
$\mathbf{t_{rv}}$: Elapsed time for relay valve
$\mathbf{t_{sim}}$: Simulation time
$\mathbf{t_{21}}$: Elapsed time for rear circuit delivery of FBV
$\mathbf{t_{22}}$: Elapsed time for rear circuit delivery of FBV
$\mathbf{V_{cl}}$: Volume of internal chamber of pipes in control line
$\mathbf{V_f}$: Volume of front brake chamber
$\mathbf{V_{max\_f}}$: Front brake chamber volume when $x_f = x_{max\ \_f}$
$\mathbf{V_{max\_r}}$: Rear brake chamber volume when $x_r = x_{max\ \_r}$
$\mathbf{V_r}$: Volume of rear brake chamber
$\mathbf{V_{rv}}$: Volume of control chamber of relay valve
$\mathbf{V_{S\_f}}$: Front supply tank volume
$\mathbf{V_{S\_r}}$: Rear supply tank volume
$\mathbf{V_{0\_f}}$: Volume of front brake chamber when $x_f = 0$
$\mathbf{V_{0\_r}}$: Volume of rear brake chamber when $x_r = 0$
$\mathbf{V_{0\_rv}}$: Volume of control chamber of relay valve when $x_{rv} = 0$
$\mathbf{V_{1\_2}}$: Internal chamber volume of pipe 1/2"
$\mathbf{V_8}$: Internal chamber volume of pipe Ø8x1
$\mathbf{V_{10}}$: Internal chamber volume of pipe Ø10x1
$\mathbf{V_{12}}$: Internal chamber volume of pipe Ø12x1.5
$\mathbf{\dot{V}_f}$: Volume rate of front brake chamber
$\mathbf{\dot{V}_r}$: Volume rate of rear brake chamber
$\mathbf{\dot{V}_{rv}}$: Volume rate of control chamber of relay valve
$\mathbf{w_f}$: Mass flow rate of front circuit
$\mathbf{w_r}$: Mass flow rate of rear circuit
$\mathbf{w_{rv}}$: Mass flow rate of relay valve
$\mathbf{x_f}$: Push rod position of front brake chamber
$\mathbf{x_{max\ \_f}}$: Maximum push rod position of front brake chamber

$\mathbf{x_{max\_r}}$: Maximum push rod position of rear brake chamber
$\mathbf{x_{max\_rv}}$: Maximum relay piston position
$\mathbf{x_r}$: Push rod position of rear brake chamber
$\mathbf{x_{rv}}$: Relay piston position
$\mathbf{x_{0\_f}}$: Initial push rod position of front brake chamber
$\mathbf{x_{0\_r}}$: Initial push rod position of rear brake chamber
$\mathbf{x_{0\_rv}}$: Initial relay piston position
$\mathbf{\dot{x}_f}$: Push rod velocity of front brake chamber
$\mathbf{\dot{x}_r}$: Push rod velocity of rear brake chamber
$\mathbf{\dot{x}_{rv}}$: Relay piston velocity
$\boldsymbol{\gamma}$: Ratio of specific heats

LIST OF TABLES

Page

LIST OF FIGURES

Page

MODELLING, ANALYSIS AND EXPERIMENTAL VERIFICATION OF PNEUMATIC BRAKE SYSTEM

SUMMARY

As the technology develops, the development in vehicle safety becomes an area, which takes the attraction of the researchers who are working in automotive industry. Although systems like air bag system, lane departure warning system (LDWS) and tire pressure monitoring system (TPMS) improve the safety of the vehicle, main studies, in which advanced technology is used mostly focus on the brake system including anti-lock braking system (ABS), traction control system (TCS), electronic stability control (ESC), advanced emergency braking system (AEBS), adaptive cruise control (ACC). Thus, detailed studies should be conducted on brake and brake system mechanism to understand, which parameters affect the braking performance of the vehicle.

Primary aim of this study is to obtain a detailed dynamic model of pneumatic brake system that will be verified with vehicle tests and be used for response time prediction on vehicle level. Secondary aim is to develop a model based design tool, which will be able to improve the response time and also the brake performance during the design stage of vehicles.

In this study, a general mathematical model is proposed to determine the dynamic characteristics of pneumatic brake system. For this purpose, first of all the details of pneumatic and mechanical subsystems of the air brake system are investigated. After that; in order to be able to execute the simulations, mathematical equations of the mechanical and pneumatic subsystems are derived and these equations are adapted to the Simulink model.

When constructing the Simulink model, some system parameters are obtained from the basic models in the literature and some are taken from the technical datasheets of the brake system components. Since a more complicated pneumatic brake system is aimed to be modeled, much more system parameters are required to be estimated. To identify those unknown parameters, response time tests were performed on a 4x4

heavy-duty vehicle equipped with wedge drum brakes. The experimental results of those tests are used to tune the system model for the unknown parameters.

For verification, simulations, which include proposed pneumatic brake system model, are performed on a different vehicle and these numerical results are verified with the vehicle tests. Here a prototype 4x4 heavy-duty vehicle equipped with disc brakes is used for the experimental study.

HAVALI FREN SİSTEMİNİN MODELLENMESİ, ANALİZİ VE DENEYSEL OLARAK DOĞRULANMASI

ÖZET

Teknolojinin artmasıyla, araç güvenliği alanındaki gelişmeler otomotiv endüstrisinde çalışmakta olan araştırmacıların dikkatini çeken bir alan haline gelmektedir. Hava yastığı sistemi, şeritten ayrılma uyarı sistemi (LDWS) ve lastik basıncı izleme sistemi (TPMS) gibi sistemler araç emniyetini arttırmasına rağmen, gelişmiş teknolojilerin kullanıldığı ana çalışmalar çoğunlukla anti-blokaj fren sistemi (ABS), çekiş kontrol sistemi (TCS), elektronik stabilite kontrolü (ESC), aktif acil frenleme sistemi (AEBS) ve adaptif hız sabitleme sistemi (ACC) gibi fren sistemi ile ilgili konulara odaklanmaktadır. Bu nedenle, aracın frenleme performansına etkiyen parametrelerin anlaşılabilmesi için fren ve fren sistemi mekanizması üzerine ayrıntılı çalışmalar gerçekleştirilmelidir.

Bu çalışmanın birincil hedefi, araç testleri ile doğrulanmış ve fren tepki süresi tahiminlerinde kullanılacak detaylı bir havalı fren sistemi dinamik modelinin elde edilmesidir. İkincil hedefi ise, araç tasarımı esnasında fren tepki süresini ve frenleme performansını arttırabilecek model tabanlı bir tasarım aracı geliştirmektir.

Bu çalışmada, havalı fren sistemi dinamik davranışını belirleyebilmek amacıyla genel bir matematiksel model önerilmektedir. Bu amaca uygun olarak, öncelikle havalı fren sisteminin pnömatik ve mekanik alt sistemlerine ait detaylar incelenmiştir. Daha sonrasında simülasyonlar için, mekanik ve pnömatik alt sistemlere ait elde edilen matematiksel ifadeler Simulink modeline uyarlanmıştır.

Simulink modelinin oluşturulması esnasında bazı sistem parametreleri literatürde bulunan temel modellerden ve bazıları ise fren sistemine ait bileşenlerin teknik veri sayfalarından elde edilmiştir. Burada daha karmaşık bir havalı fren sistemi modellemesi amaçlandığı için daha fazla sistem parametresine ihtiyaç duyulmaktadır. Bu bilinmeyen parametreleri belirleyebilmek amacıyla, fren tepki süresi testleri kamalı kampana frenli bir 4x4 ağır hizmet aracı üzerinde gerçekleştirilmiştir. Bu testlere ait deneysel sonuçlar kullanılarak sistem modelindeki bilinmeyen parametreler ayarlanmıştır.

Önerilen havalı fren sistemi modelinin doğrulanması amacıyla, farklı bir araç üzerinde simülasyonlar gerçekleştirilerek elde edilen sayısal sonuçlar araç testleri ile doğrulanmıştır. Burada, deneysel çalışma için prototip seviye disk frenli bir 4x4 ağır hizmet aracı kullanılmıştır.

1. INTRODUCTION

The brake system is one of the most critical subsystems to ensure the safety of a vehicle on road. The brake system is designed to slow down the vehicle to maintain its speed during downhill operation and to hold the vehicle stationary after it has come to a complete stop (Limpert, 1992). For the purpose of braking, kinetic energy of the vehicle is converted into the heat energy due to friction between the rotor, also called as drum or brake disc and the linings, which are the friction elements.

Two of the most commonly used actuation systems are studied: 1) The hydraulic system used on most passenger cars and light commercial vehicles and 2) The pneumatic system used on most heavy commercial and military vehicles. The hydraulic brake system was invented over 100 years ago and has been universally used in passenger cars for over 60 years. The hydraulic brake system relies upon muscular energy of the driver, which may be amplified by suitable “booster”. The basic principle of this mechanism is that incompressible brake fluid is pressurized by a “master cylinder” piston connected to the brake pedal and the pressure generated actuates foundation brake (Day, 2014).

The pneumatic brake system was fitted to most commercial and military vehicles around 60 years ago and it quickly became the standard brake system for such vehicles. It has lower cost, is more robust and it is easier to maintain than the power hydraulic system, which might be used on heavy commercial vehicles and easily accommodate electronic control (Day, 2014). Most of the tractor-trailer vehicles with a gross vehicle weight rating over 19.000 lb, most of the single trucks with a gross vehicle weight rating over 31.000 lb, most of the transit and intercity busses and about half of all school busses are equipped with air brake systems (Subramanian et al., 2003).

An effective braking mainly depends on the response time of the brake system and driver’s pedal feel. Thus, brake system layout needs to be designed by taking response time into consideration, which should meet the legal requirements and vehicle regulations. Conventionally, the brake system layout design is finalized after

many iterations based on the field trials and experiences. This increases project costs and lead time. For this reasons, the focus and the objective of this study will be to develop an accurate model of pneumatic brake system that can be widely used in the 4x4 heavy duty vehicles for purpose of the response time prediction.

There are some studies in current literature about determination of dynamic characteristic of air brake system used in vehicles.

Subramanian et al, (2003), studied on a brake system model, which predicts the pressure transients over supply pressure and partial brake applications for the operation of the primary circuit only. Once a model was developed for the pneumatic subsystem, it can be combined with a model for the mechanical subsystem to obtain a complete model of the air brake system. Pneumatic and mechanical subsystem models include foot brake valve, brake chamber and s-cam drum brake. An experimental test bench was set up and experimental data was used in order to corroborate the results, which were obtained from the model.

Subramanian et al., (2006), developed model based diagnostic schemes to automatically detect faults like leakages and out of adjustment of push rods, which can be frequently occurred in pneumatic brake system. These diagnostic schemes were studied based on pneumatic brake system model that was obtained his previous study in 2003.

Ramarathnam (2008), developed a mathematical model for leak detection in pneumatic brake system. An empirical formulation, which was expressed by using experimental mass flow rate measurements of leakage, is changed depending on supply pressure and area of leakage. The area of leakage and obtained empirical relationship were introduced into the pneumatic brake system model that was constructed in the study of Subramanian et al., (2003).

Kulesza et al., (2010), dealt with the mathematical model of the pneumatic brake system that is used in heavy trucks including the dual circuit foot brake valve and the relay valve. Some of unknown system parameters were determined by dismantling the valves used in pneumatic brake system and the others were referenced from the current literature. To be able to obtain a trustworthy model experimental investigation is required for system model verification.

He et al., (2011), investigated dynamic model of a vehicle air brake system by using standard pneumatic components, which were introduced and constructed in MWorks software. Key components of the air brake system were foot brake valve, relay valve and brake chamber. Delay time, dynamic front and rear brake chamber pressures were obtained from simulation results.

Selvaraj et al., (2014), studied on detailed pneumatic brake system model of a typical 4x2 heavy commercial vehicle by using AMESim, an integrated simulation platform designed by Siemens Company to accurately predict the multidisciplinary performance of intelligent systems. The brake system model introduced was composed of individual pneumatic brake system components as actuating valves, control valves, actuators and foundation brakes. Connections between valves were modelled by using a pneumatic pipe model including compressibility of air and friction. Response time of the system and brake torque transient were carried out for rear circuit only. The brake torque transient generated by drum brake and equivalent disc brake models were compared. When the drum brake was replaced with the disc brake, the vehicle showed better torque characteristics.

Selvaraj et al., (2014), dealt with development of pneumatic brake system model, which was constructed for the typical heavy commercial vehicle in their previous study. For the development purpose of the model, vehicle dynamics was studied by introducing road tyre interface and chassis models that have been predefined in AMESim library. Thus, stopping distance and mean fully developed deceleration (MFDD) of vehicle could be calculated. The effects caused by the engine were not taken into the consideration in the simulation. The simulation results were compared with the vehicle test results, in other words stopping distance and the MFDD.

Brubaker (2015), developed a mathematical model of pressure modulating valve that was implemented by using bond graph method. In vehicle air brake system, this type of valve is mounted on the brake pedal therefore; it is referred as a foot brake valve. The mathematical model was adapted for simulations that were performed with Matlab Simulink software. The numerical results were compared and tuned with an actual valve in order to be used to evaluate dynamic performance of the valve.

Yi et al., (2015), modelled bus pneumatic brake circuit, which includes key brake components such as foot brake valve, relay valve and diaphragm brake chamber. By

using AMESim software, it was targeted to obtain dynamic brake valve and brake chamber response curves for front and rear circuits. Pneumatic brake system test bed was designed to verify accuracy of the simulation model.

It can be shown from the literature review that ability to calculate the dynamic characteristics of pneumatic brake system is extremely important during the design phase of a new brake system. Dynamic behaviour can be obtained without the need of performing the expensive laboratory or vehicle experiments by developing a system model therefore, the verified mathematical and simulation models of the components and circuits are studied.

In this study, the primary aim is to obtain a detailed dynamic model of pneumatic brake system that will be verified with vehicle tests and be used for response time prediction on vehicle level. The secondary aim in other words the long term aim is to develop model based design tool, which is able to improve response time and also brake performance during design stage of vehicles.

In order the simulation to be trustworthy, the results of mathematical system model should reflect the experimental vehicle tests. For this reason, at the first stage of the analyses, unknown system parameters should be obtained from the experimental data taken from the vehicle tests. After tuning the unknown system parameters, at the second stage, analyses should be conducted and numerical results should be compared with experimental data, which is obtained from a different vehicle equipped with the similar brake system. If the deviation between numerical and experimental results is in acceptable limits, then the model can be considered as a good approximation of actual air brake system.

To be able to obtain a trustworthy model for prediction of the response time, following organization is taken into the consideration.

Chapter 2 describes the details of pneumatic and mechanical subsystems of the air brake system. In this chapter, the mathematical equations of the mechanical and pneumatic subsystems are derived to construct the Simulink model. Chapter 3 presents a detailed description of Simulink model of the complete pneumatic brake system regarding the mathematical equations and pneumatic service brake system layout. For the purpose of identification of unknown system parameters and verification of the Simulink model, response time tests whose details are shared in

Chapter 4 are conducted on two different 4x4 heavy-duty vehicles. Chapter 5 presents a detailed description of response time analyses that are conducted to verify Simulink model with the experimental data obtained from the vehicle tests and provides a summary of results and system improvements. Chapter 6 includes the conclusion of the study.

Before starting to model the pneumatic brake system, it is important to understand pneumatic service brake layout, usage and working principle of the components in the pneumatic brake system. Pneumatic service brake system contains front and rear supply tanks, foot brake valve, relay valve, service and spring brake chambers, pneumatic pipelines and foundation brakes.

When the driver applies the brake by pressing the brake pedal, foot brake valve opens and compressed air in supply tanks travels from the supply ports (11 and 12) to the delivery ports (21 and 22) of the foot brake valve.

For the front circuit, the compressed air flows from the delivery port of foot brake valve (22) to the input port of the quick release valve. Quick release valve divides compressed air through pneumatic pipeline into the service brake chambers mounted on the front axle.

For the rear circuit, the compressed air travels from the rear circuit delivery port of foot brake valve (21) through signal pipeline to the control port of relay valve (4). It permits to flow compressed air from supply port (1) to the delivery port (2) of relay valve. Compressed air is divided by tee passing through pneumatic pipeline and reaches into the spring brake chambers mounted on the rear axle.

Pressure in the brake chamber is converted into the force, which is transmitted to the foundation brakes in order to generate braking torque.

Service brake system layouts are shown in Figure 1.1 and 1.2 belong to the heavy-duty vehicles, on which response time tests are conducted for the verification of the pneumatic brake system model; one of the vehicles is equipped with wedge drum brakes and serial production level; the other one is equipped with disc brakes and prototype level. This layout is the key feature in the modelling procedure of the air brake system, since the effects of all components within the pneumatic brake circuit must be integrated to the mathematical model to ensure that the model is a good prediction for the actual brake system.

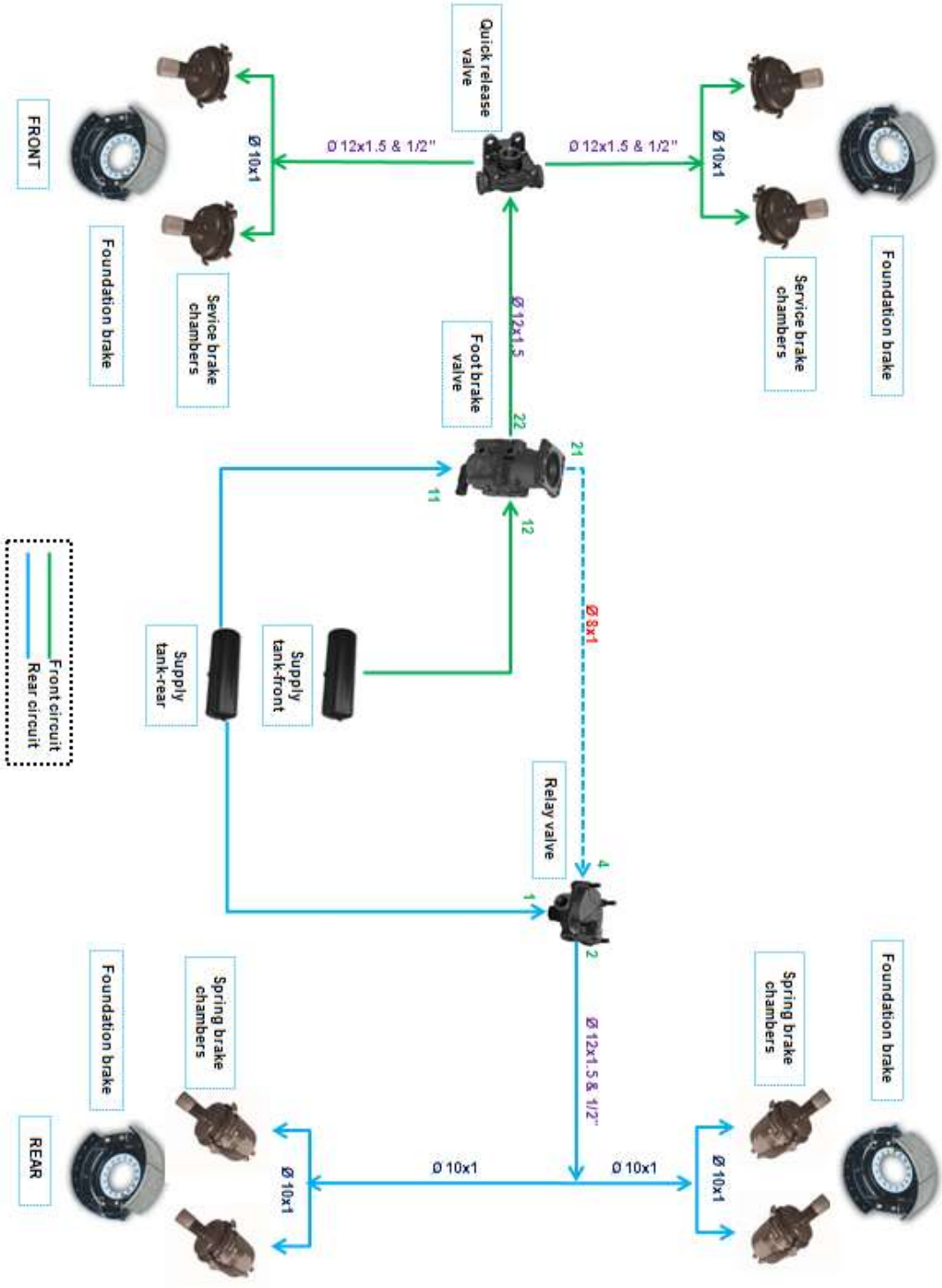

Figure 1.1 : Pneumatic service brake layout with wedge drum brakes.

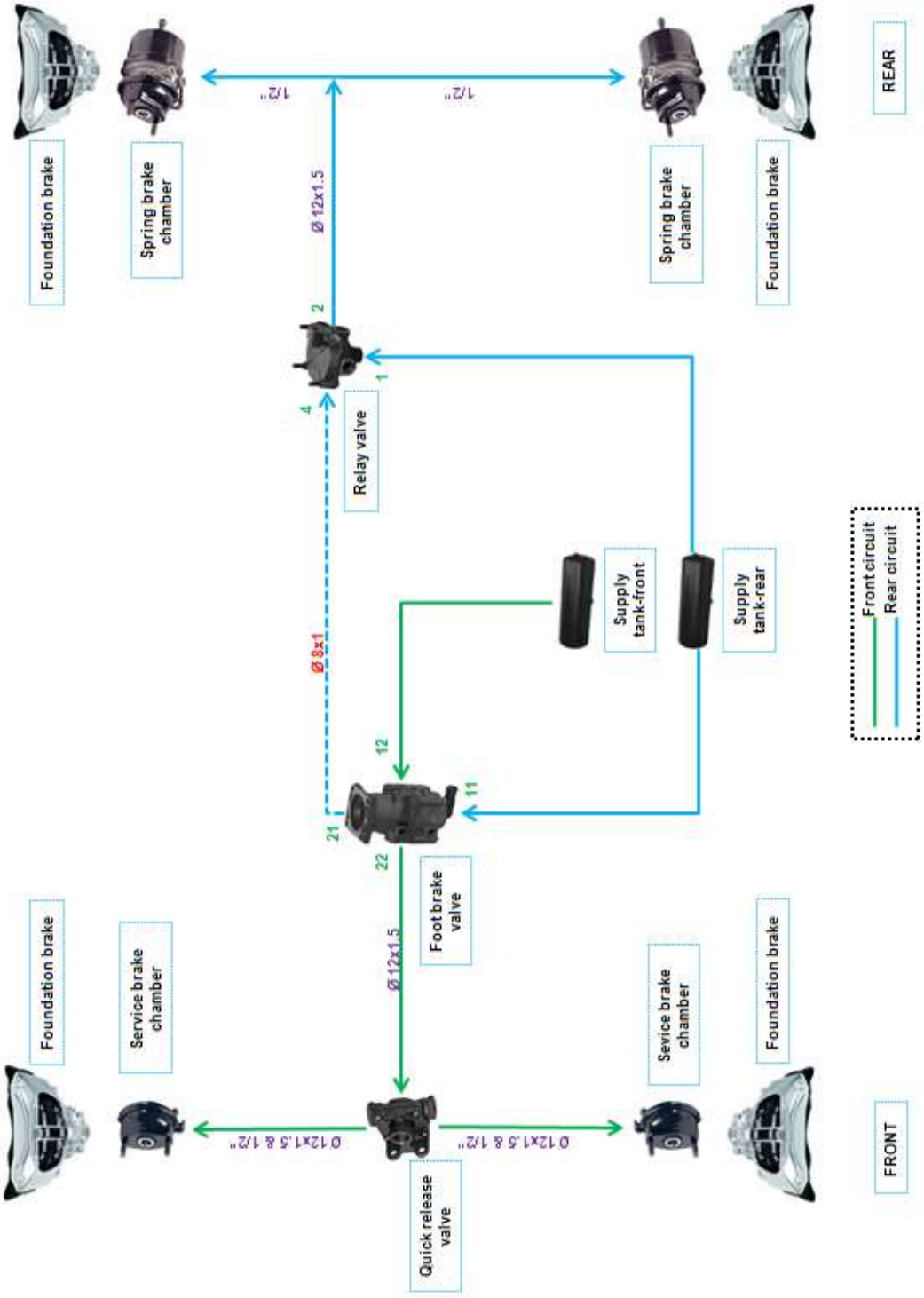

Figure 1.2 : Pneumatic service brake layout with disc brakes.

2. MATHEMATICAL MODEL

The pneumatic brake system consists of pneumatic and mechanical subsystems whose details are shown in Figure 2.1. Mechanical subsystem introduces the equations of motion related with the mechanical part of the brake system, while pneumatic subsystem deals with the dynamics of the compressible fluid, the air that is used in the brake system. Mathematical equations (2.1)-(2.25), which are used for mechanical and pneumatic subsystems are referenced from a book of Kluever, R. C., & Kluever, C. A. (2015).

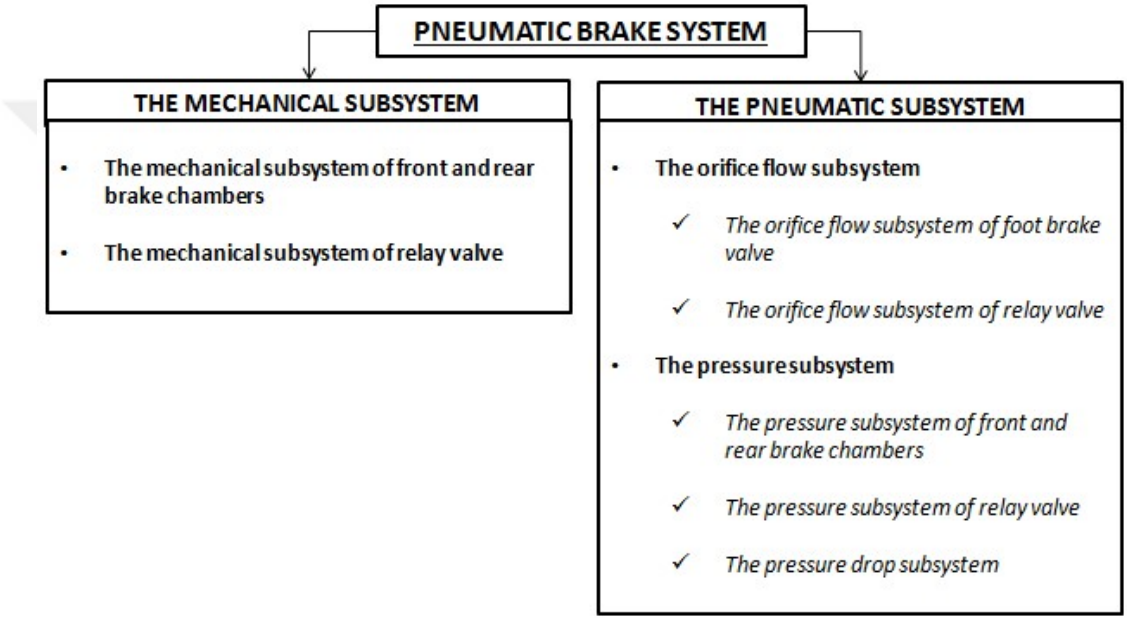

Figure 2.1 : Mechanical and pneumatic subsystem details.

2.1 The Mechanical Subsystem

When driver presses the brake pedal, foot brake valve opens and the compressed air in front and rear air tanks travels through the front and rear circuits.

For the front circuit, compressed air in front supply tank flows into the brake chamber, which is mounted on the front axle. A piston force is generated depending on pressure increase in the brake chamber and it moves the push rod to actuate the foundation brake.

For the rear circuit, compressed air in rear supply tank travels through the signal pipeline into the control port of the relay valve. Pressure increased at the control port of the relay valve moves the relay piston and it permits the compressed air to flow

from supply port of relay valve into the rear brake chamber. Pressure in the brake chamber moves the push rod to actuate foundation brake, which is mounted on the rear axle.

The mechanical subsystem can also be classified into two subsystems.

2.1.1 The mechanical subsystem of front and rear brake chambers

Figure 2.2 and 2.3 shows a free-body diagram of mechanical subsystem of front and rear brake chambers, which are composed of push rod mass, the air pressure forces, the seat contact force, the viscous friction force, the spring force with pre-load and the reactive load force due to spring in the foundation brake.

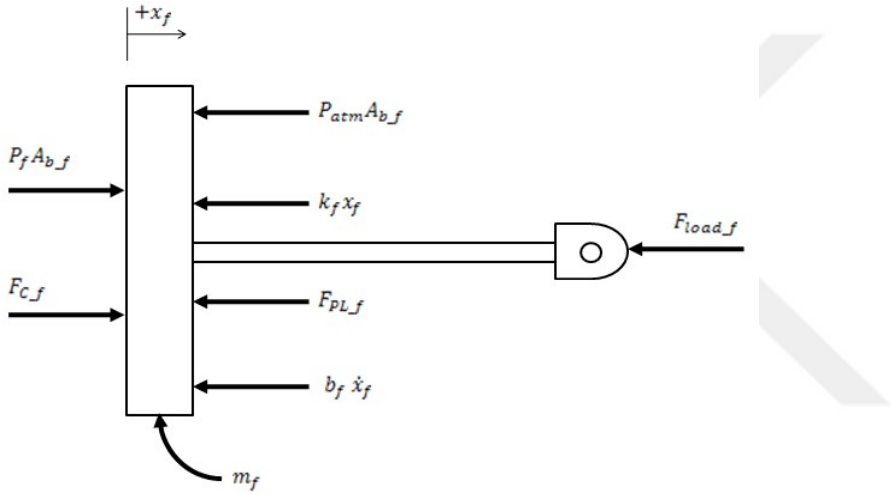

Figure 2.2 : Free-body diagram of mechanical subsystem of front brake chamber.

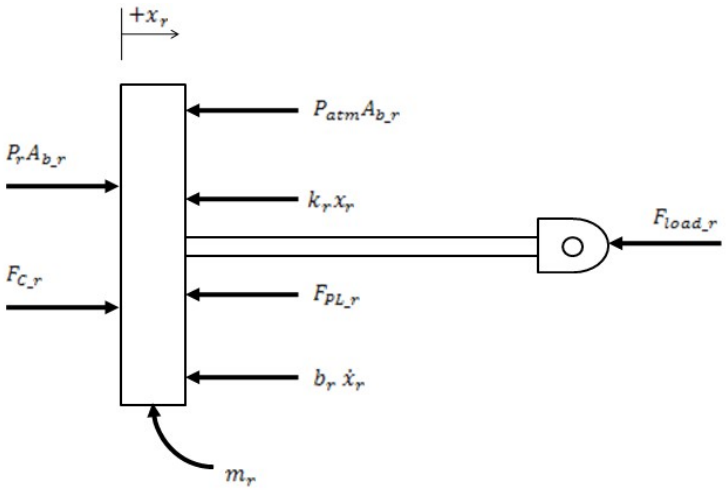

Figure 2.3 : Free-body diagram of mechanical subsystem of rear brake chamber.

Applying Newton's second law, the motion equations of mechanical subsystems can be written for front and rear brake chambers as,

$$\sum F_{front} = P_f A_{b\_f} + F_{C\_f} - P_{atm} A_{b\_f} - k_f x_f - F_{PL\_f} - b_f \dot{x}_f - F_{load\_f} = m_f \ddot{x}_f \quad \textbf{(2.1)}$$

$$\sum F_{rear} = P_r A_{b\_r} + F_{C\_r} - P_{atm} A_{b\_r} - k_r x_r - F_{PL\_r} - b_r \dot{x}_r - F_{load\_r} = m_r \ddot{x}_r \quad \textbf{(2.2)}$$

2nd order equations can be rewritten by rearranging equations (2.1) and (2.2),

$$m_f \ddot{x}_f + b_f \dot{x}_f + k_f x_f = (P_f - P_{atm}) A_{b\_f} + F_{C\_f} - F_{PL\_f} - F_{load\_f} \quad \textbf{(2.3)}$$

$$m_r \ddot{x}_r + b_r \dot{x}_r + k_r x_r = (P_r - P_{atm}) A_{b\_r} + F_{C\_r} - F_{PL\_r} - F_{load\_r} \quad \textbf{(2.4)}$$

where,

m_f, m_r: Piston/ push rod masses

b_f, b_r: Viscous friction coefficients

k_f, k_r: Return spring constants

P_f, P_r: Brake chamber pressures

P_{atm}: Atmospheric pressure

A_{b_f}, A_{b_r}: Diaphragm cross sectional areas

F_{C_f}, F_{C_r}: Seat contact forces

F_{PL_f}, F_{PL_r}: Pre load spring forces

F_{load_f}, F_{load_r}: Load forces of foundation brakes

x_f, x_r: Piston/push rod positions

$\dot{x}_f, \dot{x}_r$: Piston/push rod velocities

$\ddot{x}_f, \ddot{x}_r$: Piston/push rod accelerations

The contact force only exists when the pre-load spring force F_{PL_f} exceeds differential pressure force $(P_f - P_{atm})A_{b\_f}$. In this case, the piston is observed to be seated with $x_f = 0$. On the other hand, when differential pressure force $(P_f - P_{atm})A_{b\_f}$ exceeds pre-load spring force F_{PL_f} or $x_f > 0$ then the contact force equals to zero. Same condition is valid for rear brake chamber. This situation is described in equations (2.5) and (2.6).

$$F_{C\_f} = \begin{cases} F_{PL\_f} - (P_f - P_{atm})A_{b\_f} & \text{if} \quad F_{PL\_f} > (P_f - P_{atm})A_{b\_f} \text{ and } x_f = 0 \\ 0 & \text{if} \quad F_{PL\_f} \leq (P_f - P_{atm})A_{b\_f} \text{ or } x_f > 0 \end{cases} \quad \textbf{(2.5)}$$

$$F_{C\_r} = \begin{cases} F_{PL\_r} - (P_r - P_{atm})A_{b\_r} & \text{if} \quad F_{PL\_r} > (P_r - P_{atm})A_{b\_r} \text{ and } x_r = 0 \\ 0 & \text{if} \quad F_{PL\_r} \leq (P_r - P_{atm})A_{b\_r} \text{ or } x_r > 0 \end{cases} \quad \textbf{(2.6)}$$

2.1.2 The mechanical subsystem of relay valve

Figure 2.3 shows a free-body diagram of mechanical subsystem of relay valve, which is composed of relay piston mass, the pressure force of control port, the seat contact force, the viscous friction force and the spring force with pre-load.

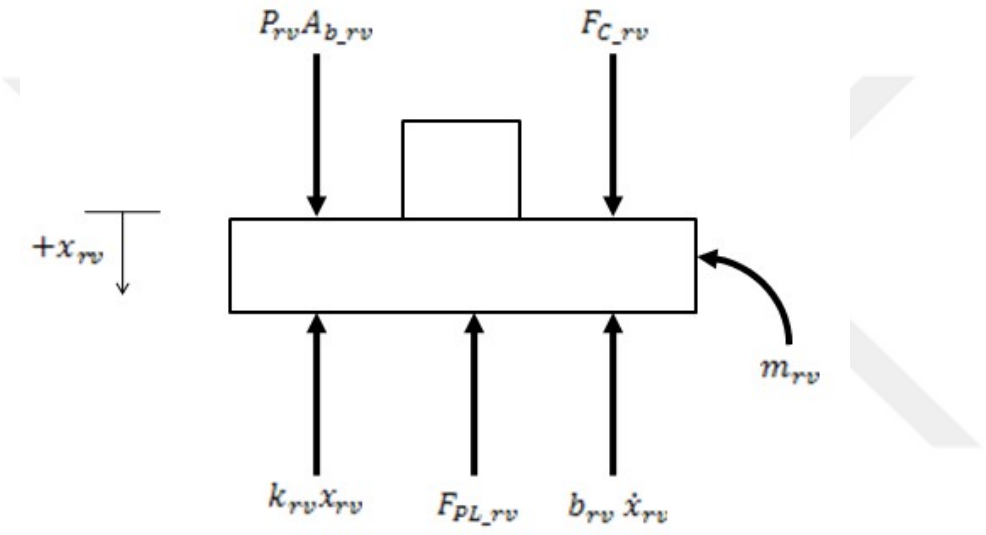

Figure 2.4 : Free-body diagram of mechanical subsystem of relay valve.

Applying Newton's second law, the equation of mechanical subsystem can be written for relay valve as,

$$\sum F_{rv} = P_{rv}A_{b\_rv} + F_{C\_rv} - k_{rv}x_{rv} - F_{PL\_rv} - b_{rv}\,\dot{x}_{rv} = m_{rv}\ddot{x}_{rv} \quad \textbf{(2.7)}$$

2nd order equation can be rewritten by rearranging equation (2.7),

$$m_{rv}\ddot{x}_{rv} + b_{rv}\dot{x}_{rv} + k_{rv}x_{rv} = P_{rv}A_{b\_rv} + F_{C\_rv} - F_{PL\_rv} \quad \textbf{(2.8)}$$

where,

m_{rv}: Relay piston mass

b_{rv}: Viscous friction coefficient of relay valve

k_{rv}: Return spring constant of relay valve

P_{rv}: Control port pressure of relay valve

A_{b_rv}: Cross sectional area of relay piston

F_{C_rv}: Seat contact force of relay valve

F_{PL_rv}: Pre load spring force of relay valve

x_{rv}: Relay piston position

$\dot{x}_{rv}$: Relay piston velocity

$\ddot{x}_{rv}$: Relay piston acceleration

The contact force only exists when the pre-load spring force F_{PL_rv} exceeds pressure force $P_{rv}A_{b\_rv}$. In this case, the piston is observed to be seated with $x_{rv} = 0$. On the other hand, when pressure force $P_{rv}A_{b\_rv}$ exceeds pre-load spring force F_{PL_rv} or $x_{rv} > 0$ then the contact force equals to zero. This situation is described in equation (2.9).

$$F_{C\_rv} = \begin{cases} F_{PL\_rv} - P_{rv}A_{b\_rv} & \text{if} \quad F_{PL\_rv} > P_{rv}A_{b\_rv} \text{ and } x_{rv} = 0 \\ 0 & \text{if} \quad F_{PL\_rv} \leq P_{rv}A_{b\_rv} \text{ or } x_{rv} > 0 \end{cases} \quad \textbf{(2.9)}$$

2.2 The Pneumatic Subsystem

The pneumatic subsystem includes the front and rear supply tank pressures, which are connected to the front and rear brake chambers passing through the foot brake valve, the relay valve (for rear circuit only) and the pneumatic pipelines. Pressing the brake pedal opens the foot brake valve. The foot brake valve modulates highly pressurized air flow from the front and rear supply tanks to the front brake chamber and control port of relay valve. Exceeding the threshold pressure of control port opens relay valve. The relay valve modulates compressed air from rear supply tank to the rear brake chamber. Brake chamber pressure alters with the change of mass flow rate and chamber volume, which is dependent to the push rod stroke.

The pneumatic subsystem can also be classified into three subsystems.

2.2.1 The orifice flow subsystem

2.2.1.1 The orifice flow subsystem of foot brake valve

Mass-flow rates of the foot brake valve front and rear circuit deliveries are modelled by the orifice flow equations, which are given below for “chocked” and “unchocked flow” conditions depending on ratios of downstream to upstream pressure.

$$w_f = C_d A_v P_{st} \sqrt{\frac{2\gamma}{(\gamma-1)RT}\left[\left(\frac{P_f}{P_{st}}\right)^{\frac{2}{\gamma}} - \left(\frac{P_f}{P_{st}}\right)^{\frac{\gamma+1}{\gamma}}\right]} \quad \text{if} \quad \frac{P_f}{P_{st}} > C_r \quad \text{(unchocked)} \quad \textbf{(2.10)}$$

$$w_f = C_d A_v P_{st} \sqrt{\frac{\gamma}{RT} C_r^{\frac{\gamma+1}{\gamma}}} \quad \text{if} \quad \frac{P_f}{P_{st}} \leq C_r \quad \text{(chocked)} \quad \textbf{(2.11)}$$

$$w_r = C_d A_v P_{st} \sqrt{\frac{2\gamma}{(\gamma-1)RT}\left[\left(\frac{P_{rv}}{P_{st}}\right)^{\frac{2}{\gamma}} - \left(\frac{P_{rv}}{P_{st}}\right)^{\frac{\gamma+1}{\gamma}}\right]} \quad \text{if} \quad \frac{P_{rv}}{P_{st}} > C_r \quad \text{(unchocked)} \quad \textbf{(2.12)}$$

$$w_r = C_d A_v P_{st} \sqrt{\frac{\gamma}{RT} C_r^{\frac{\gamma+1}{\gamma}}} \quad \text{if} \quad \frac{P_{rv}}{P_{st}} \leq C_r \quad \text{(chocked)} \quad \textbf{(2.13)}$$

where,

w_f, w_r: Mass flow rates

C_d: Discharge coefficient of FBV

A_v: Orifice cross sectional area of FBV

P_{st}: Steady state system pressure

γ: Ratio of specific heats $(\gamma_{air} = 1.4)$

R: Gas constant

T: Air temperature

C_r: Critical pressure ratio

Critical pressure ratio can be written as a function of ratio of specific heats,

$$C_{r=} \left(\frac{2}{\gamma+1}\right)^{\frac{\gamma}{\gamma-1}} \quad \textbf{(2.14)}$$

The critical pressure ratio is equal to 0.528 for air. When ratio of the downstream to upstream pressure (i.e. ratio of P_f to P_{st} for front circuit) is greater than the critical pressure ratio, then subsonic "unchocked flow" occurs at the valve orifice. On the other side when the critical pressure ratio of air is greater than the ratio of downstream to upstream pressure, then sonic (Mach 1) "chocked flow" involves at the valve orifice.

2.2.1.2 The orifice flow subsystem of relay valve

Mass-flow rate of relay valve is modelled by the orifice flow equations, which are given below for "chocked" and "unchocked flow" conditions depending on ratios of downstream to upstream pressure.

$$w_{rv} = C_{d\_rv}\, A_{v\_rv}\, P_{st} \sqrt{\frac{2\gamma}{(\gamma-1)RT}\left[\left(\frac{P_r}{P_{st}}\right)^{\frac{2}{\gamma}} - \left(\frac{P_r}{P_{st}}\right)^{\frac{\gamma+1}{\gamma}}\right]} \quad \text{if} \quad \frac{P_r}{P_{st}} > C_r \quad \text{(unchocked)} \tag{2.15}$$

$$w_{rv} = C_{d\_rv}\, A_{v\_rv}\, P_{st} \sqrt{\frac{\gamma}{RT} C_r^{\frac{\gamma+1}{\gamma}}} \quad \text{if} \quad \frac{P_r}{P_{st}} \leq C_r \quad \text{(chocked)} \tag{2.16}$$

where,

w_{rv}: Mass flow rate of relay valve

C_{d_rv}: Discharge coefficient of relay valve

A_{v_rv}: Orifice cross sectional area of relay valve

2.2.2 The pressure subsystem

2.2.2.1 The pressure subsystem of front and rear brake chambers

Using basic modelling equation for pneumatic system, 1st order pressure equations can be written for front and rear brake chambers as,

$$\dot{P}_f = \frac{nRT}{V_f}\left(w_f - \frac{P_f}{RT}\dot{V}_f\right) \tag{2.17}$$

$$\dot{P}_r = \frac{nRT}{V_r}\left(w_{rv} - \frac{P_r}{RT}\dot{V}_r\right) \tag{2.18}$$

where,

$\dot{P}_f, \dot{P}_r$: Pressure rates

n: Exponent of polytropic expansion process

V_f, V_r: Volumes of brake chambers

Exponent of polytrophic expansion process is assumed as value of $n = 1$ because of isothermal process.

Brake chamber volumes can be written as function of push rod positions x_f and x_r,

$$V_f = V_{0\_f} + A_{b\_f} x_f \tag{2.19}$$

$$V_r = V_{0\_r} + A_{b\_r} x_r \quad \textbf{(2.20)}$$

where V_{0_f} and V_{0_r} are the volumes when push rod positions $x_f = 0$ and $x_r = 0$.

Time derivatives of brake chamber volumes can be written as function of push rod velocities $\dot{x}_f$ and $\dot{x}_r$,

$$\dot{V}_f = A_{b\_f}\, \dot{x}_f \quad \textbf{(2.21)}$$

$$\dot{V}_r = A_{b\_r}\, \dot{x}_r \quad \textbf{(2.22)}$$

2.2.2.2 The pressure subsystem of relay valve

1st order pressure equation of relay valve is given below.

$$\dot{P}_{rv} = \frac{nRT}{V_{rv}}\left(w_r - \frac{P_{rv}}{RT}\dot{V}_{rv}\right) \quad \textbf{(2.23)}$$

where,

$\dot{P}_{rv}$: Pressure rate of control chamber

V_{rv}: Control chamber volume of relay valve

Control chamber volume of relay valve can be written as function of relay piston position x_{rv},

$$V_{rv} = V_{0\_rv} + V_{cl} + A_{b\_rv}\, x_{rv} \quad \textbf{(2.24)}$$

where,

V_{0_rv}: Control chamber volume when $x_{rv} = 0$

V_{cl}: Volume of internal chamber of pipes in control line

Time derivative of control chamber volume can be written as function of relay piston velocity $\dot{x}_{rv}$,

$$\dot{V}_{rv} = A_{b\_rv}\, \dot{x}_{rv} \quad \textbf{(2.25)}$$

2.2.2.3 The pressure drop subsystem

Pressing the brake pedal opens the foot brake valve and pressurized air in front and rear supply tanks starts to fill the brake chambers, passing through pneumatic pipelines by increasing total amount of volume. Because of this reason, air pressure in front and rear supply tanks decreases until reaching the steady state pressure of the pneumatic brake system.

Applying Boyle's gas law, the equation of pressure drop subsystem can be written as,

$$P_{S_f}V_{S_f} + P_{S_r}V_{S_r} = P_{st}(V_{S\_f} + V_{S\_r} + n_f V_{max\ \_f} + n_r V_{max\_r} + V_8 + V_{10} + V_{12} + V_{1\_2}) \quad \textbf{(2.26)}$$

where,

P_{S_f}: Front supply tank pressure

P_{S_r}: Rear supply tank pressure

V_{S_f}: Front supply tank volume

V_{S_r}: Rear supply tank volume

V_{max_f}: Front brake chamber volume when $x_f = x_{ma\ \_f}$

V_{max_r}: Rear brake chamber volume when $x_r = x_{max\ \_r}$

n_f: Number of brake chamber at front axle

n_r: Number of brake chamber at rear axle

V_8: Internal chamber volume of pipe Ø8x1

V_{10}: Internal chamber volume of pipe Ø10x1

V_{12}: Internal chamber volume of pipe Ø12x1.5

V_{1_2}: Internal chamber volume of pipe 1/2"

Pressure drop in front and rear circuits can be written as,

$$dP_f = P_{S\_f} - P_{st} \quad \textbf{(2.27)}$$

$$dP_r = P_{S\_r} - P_{st} \quad \textbf{(2.28)}$$

3. SIMULINK MODEL

In this study, Matlab Simulink software is used in order to construct and develop the complete pneumatic brake system model.

Figure 3.1 shows Simulink model of pneumatic brake system, which is developed according to the mathematical equations mentioned for mechanical and pneumatic subsystems in Chapter 2. Pneumatic front and rear circuits in service brake system layout are included into the model.

In complete system model, one of the system inputs is defined as a step function of driver's brake pedal force F_{pedal} and the other inputs are defined as front and rear circuit's supply pressures P_{S_f} and P_{S_r}, which are constant. Valve's orifice cross sectional area A_v is proportional to the driver's brake pedal force F_{pedal} therefore; it is defined as a gain factor in Simulink model.

Mechanical and brake chamber pressure subsystem blocks are generated for front and rear brake chambers and relay valve.

Regarding the 2^{nd} order equations of the mechanical subsystem of front and rear brake chambers, there are two state variables for each brake chamber. Those are push rod positions and their time derivatives; in other words x_f, $\dot{x}_f$ for front brake chamber and x_r, $\dot{x}_r$ for rear brake chamber. Brake chamber pressures P_f and P_r, providing actuation forces of the foundation brakes are the input variables.

In mechanical subsystem of relay valve; relay piston position x_{rv} and relay piston velocity $\dot{x}_{rv}$ are output variables and control port pressure of relay valve P_{rv} is the single input.

Orifice flow subsystem blocks are constructed for foot brake and relay valves. In orifice flow subsystem of the foot brake valve; supply tank pressures P_{S_f} and P_{S_r}, orifice cross sectional area of foot brake valve A_v, front brake chamber pressure P_f, control port pressure of relay valve P_{rv}, pressure drop in front and rear circuits dP_f and dP_r are input variables and mass flow rates w_f and w_r are output variables.

In orifice flow subsystem of relay valve; rear supply tank pressure P_{S_r}, orifice cross sectional area of relay valve A_{v_rv}, pressure drop in rear circuit dP_r and rear brake

chamber pressure P_r are input variables and mass flow rate of relay valve w_{rv} is single output.

Pressure subsystem blocks are generated for front and rear brake chambers and relay valve. In pressure subsystem of front and rear brake chambers; brake chamber pressures P_f and P_r are defined as output variables regarding the 1st order pressure equation. Push rod positions x_f and x_r, push rod velocities $\dot{x}_f$ and $\dot{x}_r$, mass flow rate of front circuit w_f and mass flow rate of relay valve w_{rv} are input variables. Brake chamber volumes V_f and V_r and their time derivatives $\dot{V}_f$ and $\dot{V}_r$ are computed by using push rod positions x_f and x_r and push rod velocities $\dot{x}_f$ and $\dot{x}_r$, which are given in equations (2.21) and (2.22).

In pressure subsystem of relay valve; mass flow rate of rear circuit w_r, relay piston position x_{rv} , and its time derivative $\dot{x}_{rv}$ are input variables and control port pressure of relay valve P_{rv} is output variable. Control chamber volume V_{rv} and its time derivative $\dot{V}_{rv}$ are calculated by relay piston position x_{rv} and relay piston velocity $\dot{x}_{rv}$.

When control port pressure of relay valve P_{rv} exceeds its threshold value of P_{th_rv} then orifice cross sectional area of relay valve switches zero to A_{v_rv} therefore, a switch block is added into the complete system model as a decision signal.

Regarding Boyle's gas law equations of the pressure drop subsystem; there are two outputs, which are pressure drop in front and rear circuits dP_f and dP_r .

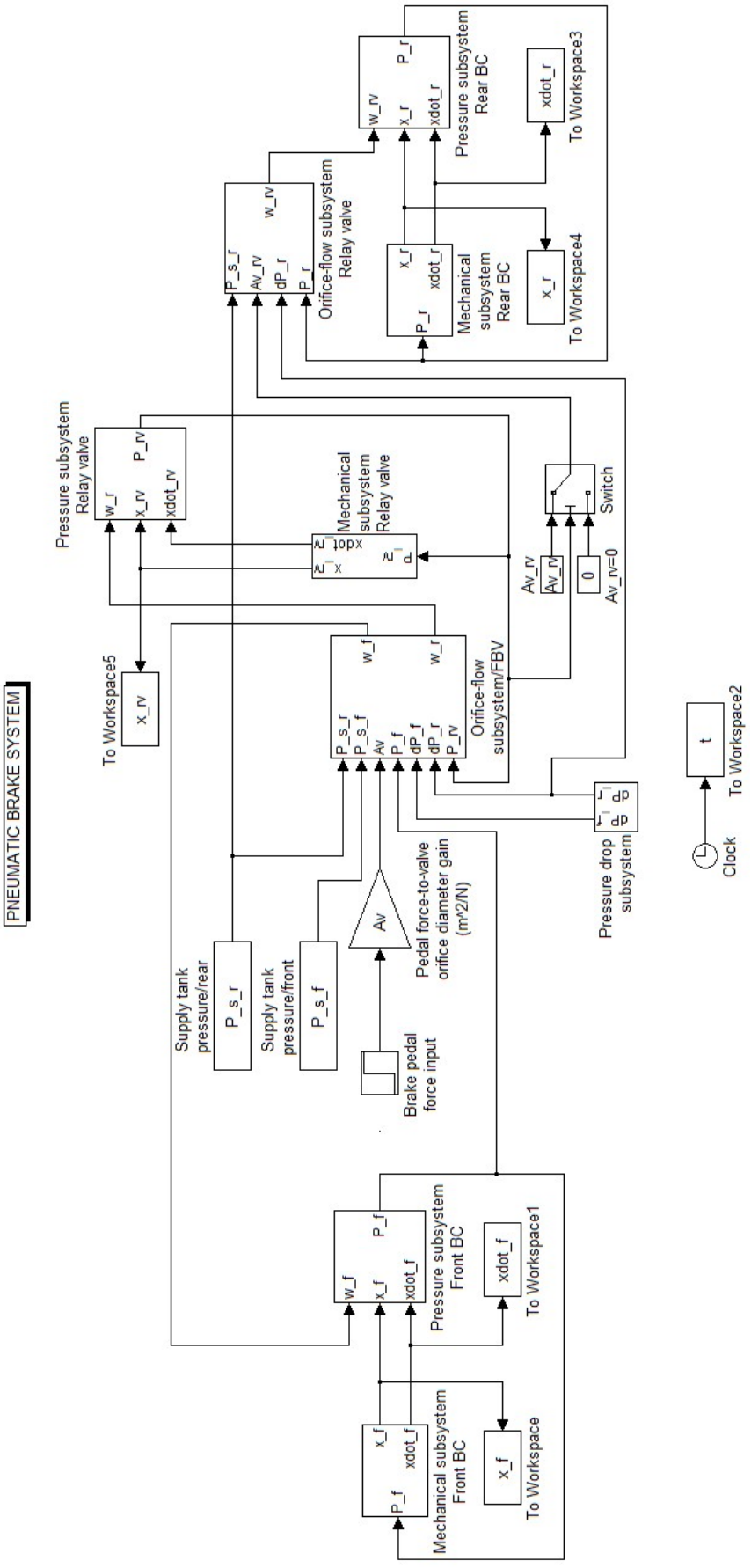

Figure 3.1 : Simulink model of pneumatic brake system.

3.1 The Mechanical Subsystem Blocks

Mechanical subsystem blocks of front and rear brake chambers are constructed to introduce equations (2.3) and (2.4) into the model. Inner details of mechanical subsystem of front and rear brake chambers are shown in Figure 3.2 and 3.3.

First dashed box in Figure 3.2 shows contact force calculation, which is expressed in equation (2.5) and (2.6) for front and rear brake chambers. A saturation block is used for determining lower and upper limits of the difference between differential pressure force $(P_f - P_{atm})A_{b\_f}$ and pre-load spring force F_{PL_f}. The contact force F_{C_f} can only take a positive value for this reason; lower limit of saturation block is defined as zero. The contact force F_{C_f} only exists when piston is seated or piston position is zero therefore, a switch block is added into the model as a decision signal.

Second dashed box in Figure 3.2 indicates the hard stop limit philosophy of push rod. Push rod displacement x_f cannot exceed maximum push rod displacement $x_{max\ \_f}$ because of full engagement of linings and disc or drum. When integrator output x_f has reached its limit $x_{max\ \_f}$ then push rod velocity $\dot{x}_f$ is equal to 0 and saturation signal indicates a value of 1. Logical operator block is set to NOT operation and it converts the saturation signal from 1 to 0. This obtained output signal is multiplied by the velocity signal of the push rod $\dot{x}_f$ to produce push rod velocity information for being used in the simulation. On the other hand, when integral has not reached its limit then saturation signal is equals to 0 and it is converted from 0 to 1 by NOT operation.

The load force of the foundation brake F_{load_f} only exists when push rod displacement is greater than zero. For this reason, a switch is added to the mechanical subsystem of front brake chamber that is shown as third dashed box in Figure 3.2.

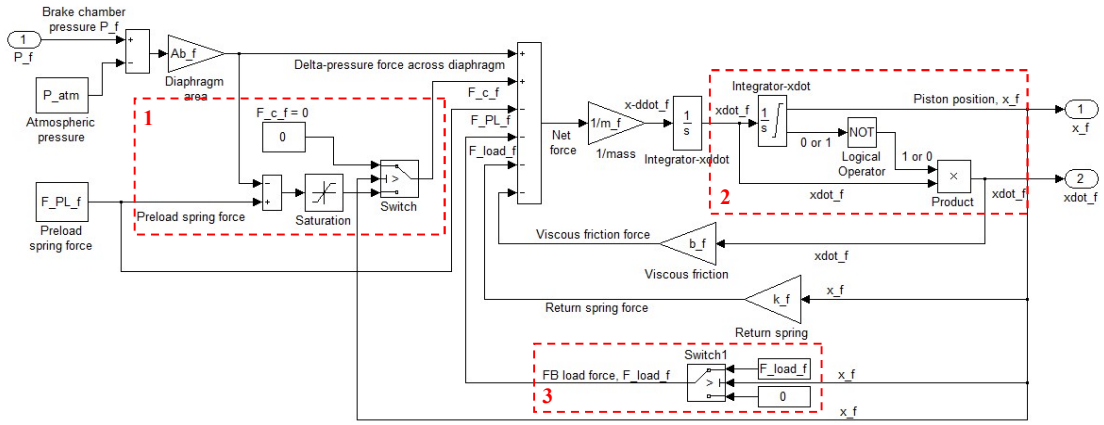

Figure 3.2 : Mechanical subsystem of front brake chamber.

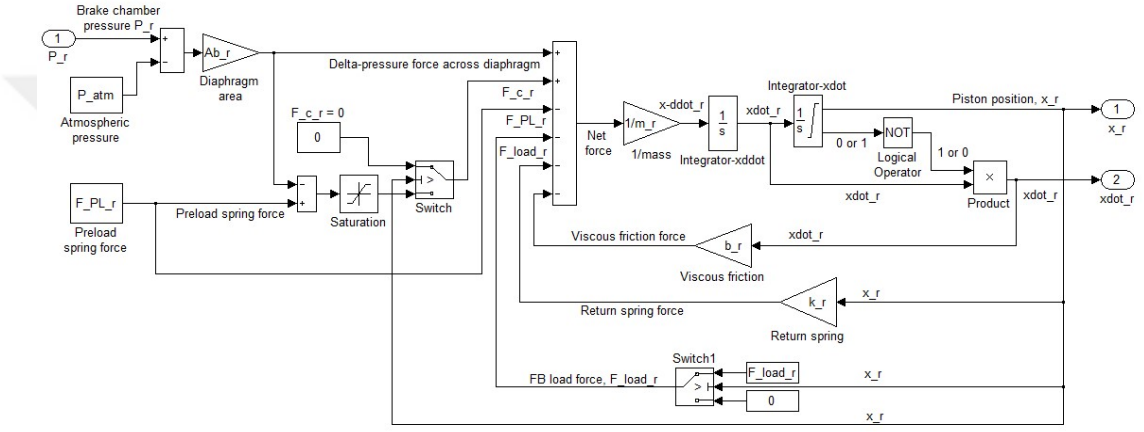

Figure 3.3 : Mechanical subsystem of rear brake chamber.

Mechanical subsystem block of relay valve is constructed for the integration of equation (2.8) to the model. Inner details of mechanical subsystem of relay valve are shown in Figure 3.4.

First dashed box in Figure 3.4 shows contact force calculation, which is expressed in equation (2.9) for relay valve. A saturation block is used for determining lower and upper limits of the difference between pressure force $P_{rv}A_{b\_rv}$ and pre-load spring force F_{PL_rv}. The contact force F_{C_rv} can only take a positive value, for this reason, lower limit of saturation block is defined as zero. The contact force F_{C_rv} only exists when piston is seated or piston position is zero therefore, a switch block is added into the model as a decision signal.

Second dashed box in Figure 3.4 indicates the hard stop limit philosophy of relay piston. Relay piston displacement x_{rv} cannot exceed maximum relay piston displacement x_{max_rv}. When integrator output x_{rv} has reached its limit x_{max_rv}, then relay piston velocity $\dot{x}_{rv}$ is equal to 0 and saturation signal indicates a

value of 1. Logical operator block is set to NOT operation and it converts the saturation signal from 1 to 0. This obtained output signal is multiplied by the velocity signal of the relay piston $\dot{x}_{rv}$ to produce relay piston velocity information for being used in the simulation. On the other hand, when integral has not reached its limit then saturation signal is equals to 0 and it is converted from 0 to 1 by NOT operation.

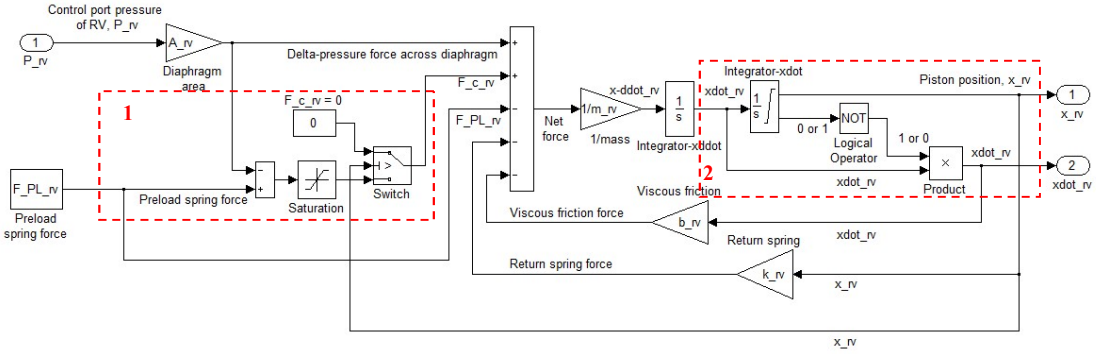

Figure 3.4 : Mechanical subsystem of relay valve.

3.2 The Pneumatic Subsystem Blocks

3.2.1 The orifice flow subsystem blocks

Details of orifice flow subsystem of foot brake valve are shown in Figure 3.5. Interpreted MATLAB Fcn blocks are defined to calculate mass flow rate of front and rear circuits w_f and w_r for chocked and unchocked flow conditions. For this purpose, customized M-files *Valve_front.m* and *Valve_rear.m* are generated by using equations (2.10)-(2.14). Foot brake valve is actuated by pressing the pedal and due to this action; predominance is occurred between front and rear circuit deliveries depending on the characteristic curve of valve. When control port pressure of relay valve P_{rv} is greater than predominance pressure value of foot brake valve P_{FBV}, then orifice cross sectional area of the front circuit switches zero to A_v . For this reason, a switch block is added to the orifice flow subsystem of foot brake valve.

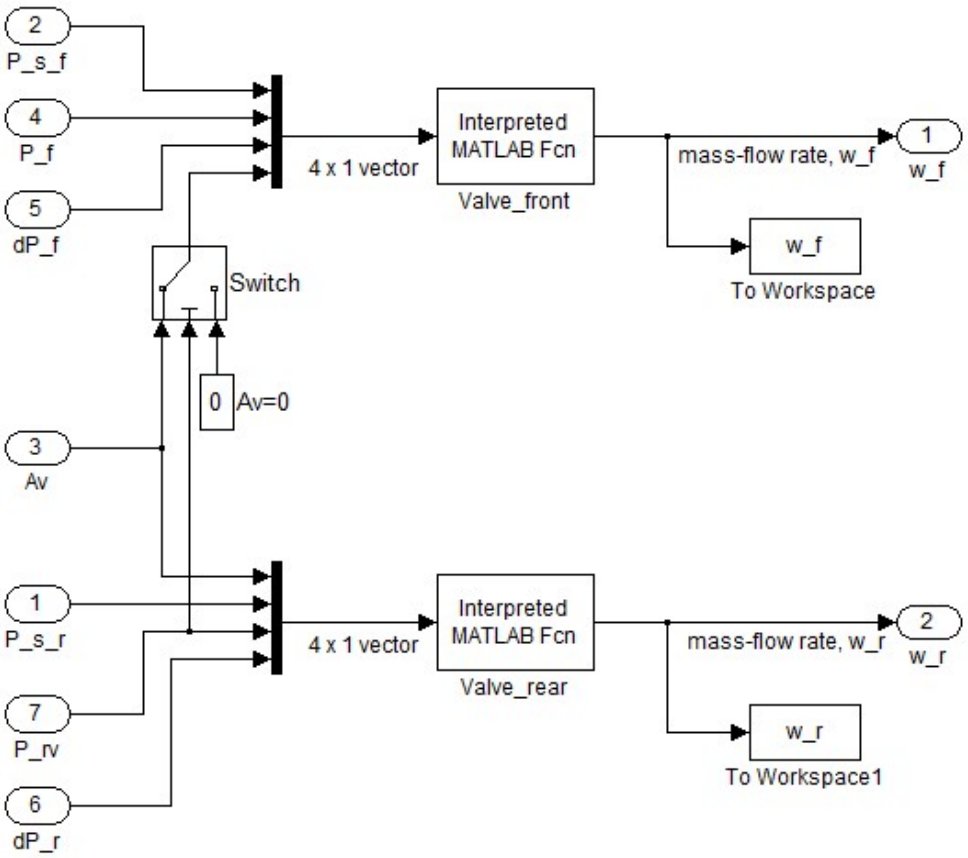

Figure 3.5 : Orifice flow subsystem of foot brake valve.

Details of orifice flow subsystem of relay valve are shown in Figure 3.6. Interpreted MATLAB Fcn block is defined to calculate mass flow rate of relay valve w_{rv} therefore, customized M-file *Valve_rv.m* is generated by using equations (2.14)-(2.16).

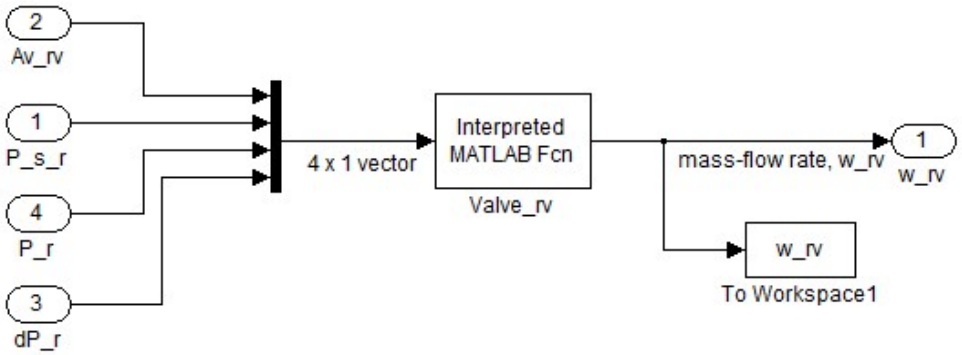

Figure 3.6 : Orifice flow subsystem of relay valve.

3.2.2 The pressure subsystem blocks

Figure 3.7 and 3.8 show the inner details of pressure subsystem blocks of front and rear brake chambers. User defined Interpreted MATLAB Fcn blocks are added by

using customized M-files *Pdot_front.m* and *Pdot_rear.m;* which contain pressure rate, volume and volume rate equations (2.17)-(2.22).

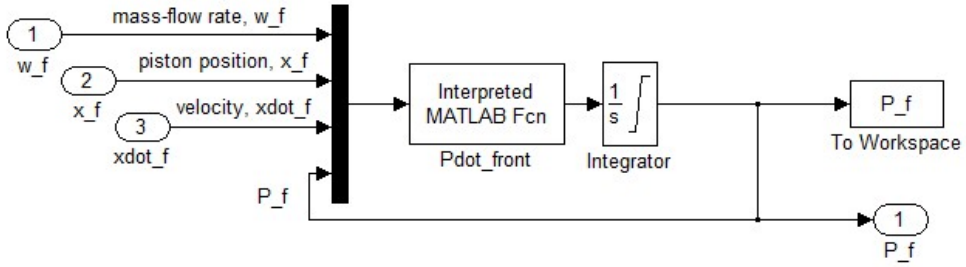

Figure 3.7 : Pressure subsystem of front brake chamber.

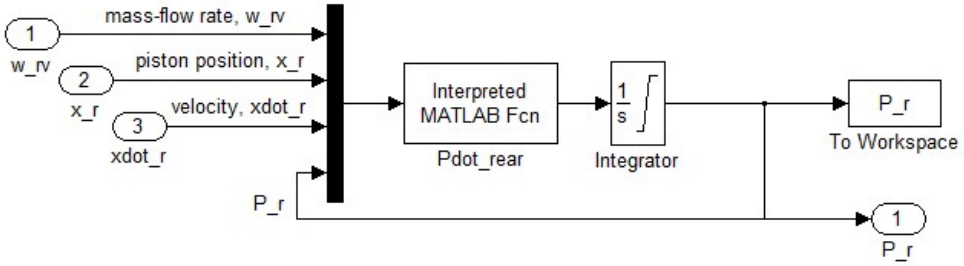

Figure 3.8 : Pressure subsystem of rear brake chamber.

Inner details of pressure subsystem block of relay valve are shown in Figure 3.9. User defined Interpreted MATLAB Fcn block is added and customized M-files *Pdot_rv.m* is generated by related equations (2.23)-(2.25).

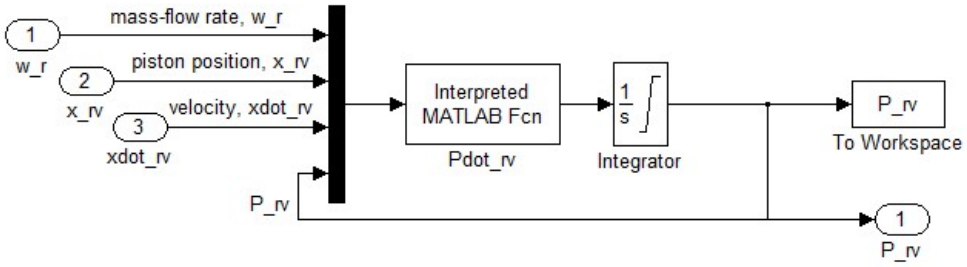

Figure 3.9 : Pressure subsystem of relay valve.

Pressure drop subsystem block is constructed for definition of equations (2.26)-(2.28) into the model. Inner details of pressure drop subsystem are shown in Figure 3.10.

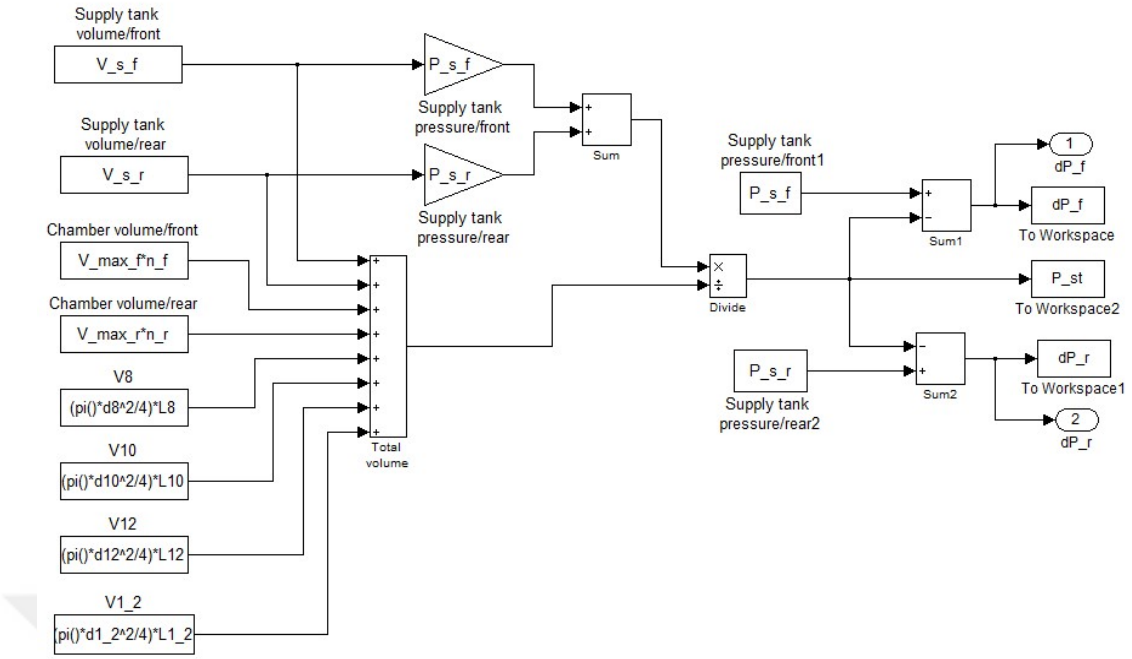

Figure 3.10 : Pressure drop subsystem.

4. EXPERIMENTAL STUDY

In this chapter, two response time tests are conducted; one for identification of the system parameters and the other for validation of the Simulink model. Tests are performed on two different heavy-duty vehicles given the details below.

4.1 Test-1: Serial Production Vehicle

Test-1 is conducted on the serial production vehicle whose air system's working pressure is equal to 8 bars. The vehicle is equipped with the wedge drum brakes. Test-1 is performed to identify and define the unknown system parameters (orifice cross sectional areas of FBV and RV, threshold pressure of RV etc.) that cannot be obtained from the technical datasheets of the air brake system components.

In order to get the response time measurements of the vehicle equipped with drum brakes, DEWESoft SIRIUSi 8xSTGM data acquisition system is installed on the vehicle as shown in Figure 4.1 below.

Figure 4.1 : Data acquisition system.

To measure brake chamber pressure transients, two Keller PR-23 SY (0-10 bar and 0-5V) pressure sensors are mounted on the brake chambers that are located at the front axle left and rear axle right as shown in Figure 4.2 and Figure 4.3.

Figure 4.2 : Pressure sensor mounted on the front axle left.

Figure 4.3 : Pressure sensor mounted on the rear axle right.

The other two pressure sensors are fitted on the front and rear circuit deliveries of the foot brake valve (Port 22 and Port 21) to measure the time elapsing from the initiation of brake pedal actuation, see Figure 4.4.

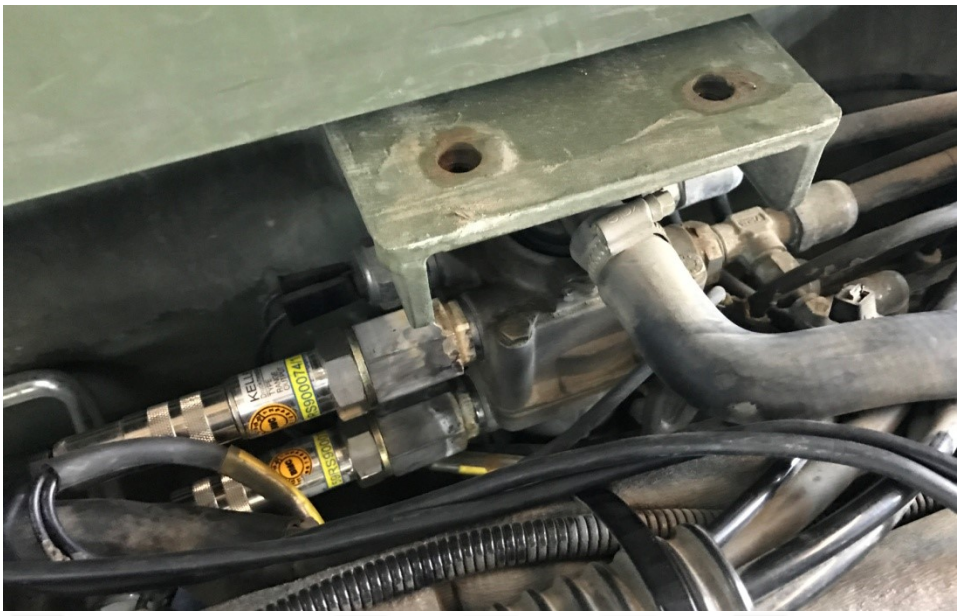

Figure 4.4 : Pressure sensors fitted on the foot brake valve.

In addition to these, two more pressure sensors are fitted on the air tanks for the purpose of monitoring front and rear tank pressures as shown in Figure 4.5.

Figure 4.5 : Pressure sensors mounted on the front and rear tanks.

All the 6 pressure sensors are connected to the DEWESoft SIRIUSi 8xSTGM data acquisition system via 6 channels and the data acquisition system is also connected to the laptop computer. Thus, the test measurements can be monitored on the laptop computer in real time. The pressure information measured by Keller PR-23 SY pressure sensors is transferred to the DEWESoft SIRIUSi 8xSTGM data acquisition system. The DEWESoftX data acquisition software stores the data in DEWESoftX

data file format. Sampling rate is set to 2000 Hz from the DEWESoftX data acquisition software. Figure 4.6 shows the DEWESoftX user interface design, which is prepared and developed for this study. The pressure information that is read by all the 6 pressure sensors depending on the elapsed time can be monitored from the digital indicators, which located on the DEWESoftX user interface.

Before the response time test, it is necessary to define cut-in pressure of the air compressor on the vehicle because at the beginning of the response time test, the pressure in the front and rear tanks must be equal to the cut-in pressure of air compressor.

Here, response time is defined as the elapsed time measured from the instant that actuation of the brake pedal is started to the instant that the pressure in the brake chamber reaches to 75% of the cut-in pressure of the air compressor (UN, 2014).

In order to define cut-in pressure of the air compressor, the following steps are taken into consideration;

1. Start the measurement and recording by using DEWESoftX software.

2. Start the engine and ensure that the vehicle is stationary and running at the idle speed.

3. Wait until the pressures in the air tanks reach cut-off pressure of air compressor.

4. Press the brake pedal at half stroke and monitor the pressure decreased in the air tanks.

5. Repeat step 4 until the pressures in the air tanks increase again (cut-in pressure of air compressor).

6. Stop data logging and review the results.

It can be seen in Figure 4.7 that the cut-in pressure of air compressor is obtained a value of 7.3 bars. Thus, 75% of the cut-in pressure of the air compressor is calculated 5.5 bars for response time determination.

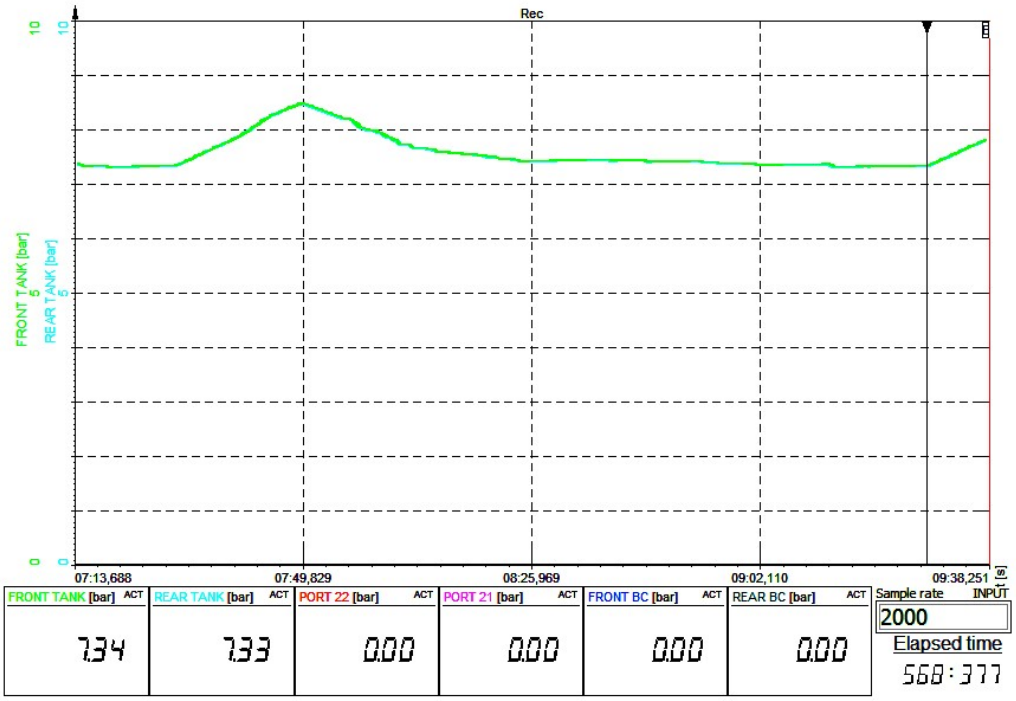

Figure 4.6 : Cut-in pressure of compressor of serial production vehicle.

The response time test procedure is as follows;

1. Start the measurement by using DEWESoftX.

2. Start the engine.

3. Release the hand brake valve.

4. Ensure that the vehicle is stationary and running at the idle speed.

5. Wait until the pressures in the air tanks reach cut-off pressure of air compressor.

6. Stop the engine.

7. Press the brake pedal at half stroke and monitor the pressure decreased in the air tanks.

8. Repeat step 7 until the pressures in the air tanks is equal to the cut-in pressure of air compressor.

9. Start recording the test by using DEWESoftX.

10. Press the brake pedal at full stroke immediately.

11. Hold the brake pedal at the end of the pedal travel.

12. Release the brake pedal immediately.

13. Stop data logging and review the results.

According to European Braking Regulation UNECE R13, following requirements must be achieved (UN, 2014).

• In order to obtain a succeeded actuation in the response time test, the pressure at the front and rear circuit deliveries of the foot brake valve must reach at some specific percentage of its asymptotic/final value at the corresponding time instants. These specific percentages and related time instants are given in Table 4.1.

• For an actuating time of 0.2 seconds, response time should not exceed 0.6 s and response time measurement results should be rounded to the nearest tenth of a second.

Table 4.1 : Requirements of a succeeded actuation (UN, 2014).

.. (%) of asymptotic/final value	Elapsed time (s)
10	**0.2**
75	**0.4**

Figure 4.7 shows response time test results of serial production vehicle. It can be seen that final pressure at the front and rear circuit deliveries of the foot brake valve is equal to 6.6 bars.

Here, the elapsed time measured from the actuation of brake pedal to the time that the pressure reaches to 10% of final pressure of the front delivery is equal to t_{22} =0.02 s. As for the rear delivery, the elapsed time is monitored as t_{21} =0.01 s.

For the second requirement of a succeeded actuation, the elapsed time measured from the actuation of brake pedal to the time that the pressure reaches to 75% of final pressure of the front delivery is equal to t_{22} =0.4 s. As for the rear delivery, the elapsed time is monitored as t_{21} =0.1 s. Therefore, results of response time test fulfill the requirements of a succeeded actuation.

For the response time determination, 75% of the cut-in pressure of the air compressor is obtained 5.5 bars. At this point, response time results of front and rear brake chambers are obtained as t_f =0.6 s and t_r =0.5 s respectively. Hence, it can be concluded that for the given test requirements response time results of front and rear circuits stay within regulation limits.

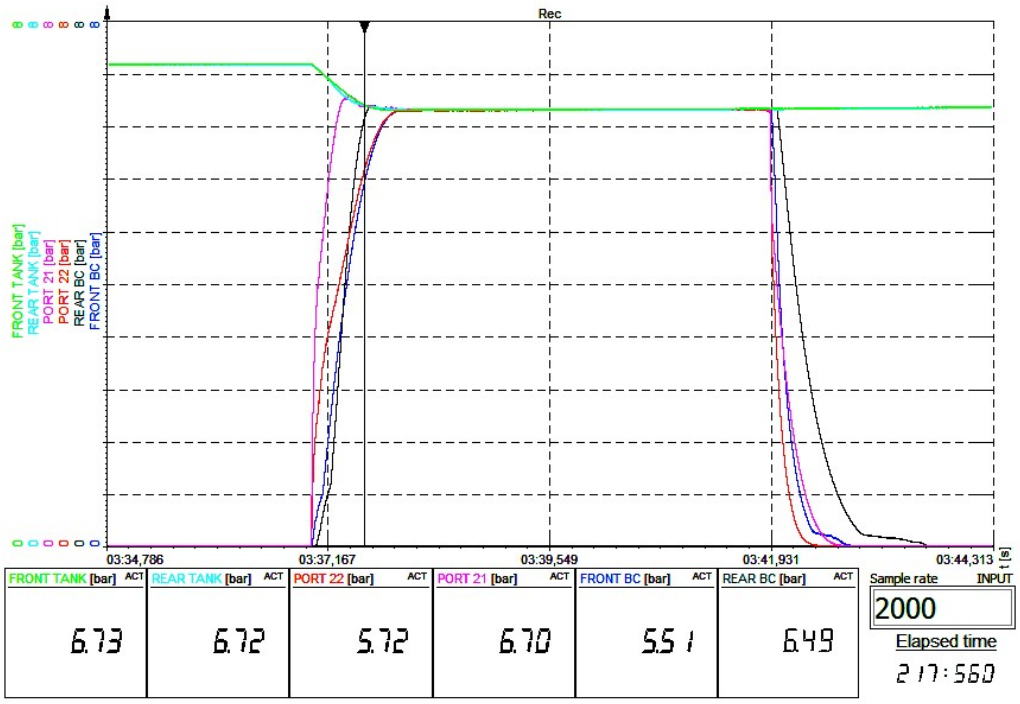

Figure 4.7 : Response time test results of serial production vehicle.

4.2 Test-2: Prototype Vehicle

Test-2 is performed on the prototype vehicle whose working pressure is equal to 10 bars. The vehicle is equipped with the disc brakes. Test-2 is conducted for the verification and validation of pneumatic brake system model, which is constructed and developed in this study to predict response time of the system. For this purpose, DEWESoft SIRIUSi 8xSTGM data acquisition system is installed on the vehicle.

As mentioned in Test-1, all the 6 pressure sensors are connected to the DEWESoft SIRIUSi 8xSTGM data acquisition system. Two pressure sensors (Keller PR-23 SY 0-10 bar and 0-5 V) that are used to measure the front and rear brake chambers' pressures located at the front axle left and rear axle left as shown in Figure 4.8 and Figure 4.9. Other two pressure sensors are fitted on the front and rear circuit deliveries of the foot brake valve (Port 22 and Port 21), see Figure 4.10. Furthermore, two pressure sensors, which are used for monitoring the front and rear tank pressures, are mounted on the air tanks, as shown in Figure 4.11.

Figure 4.8 : Pressure sensor mounted on the front axle left of prototype vehicle.

Figure 4.9 : Pressure sensor mounted on the rear axle left of prototype vehicle.

Figure 4.10 : Pressure sensors mounted on the foot brake valve of prototype vehicle.

Figure 4.11 : Pressure sensors mounted on the front and rear tanks of prototype vehicle.

Cut-in pressure of air compressor is obtained as 8.8 bars by repeating test for the prototype vehicle using cut-in pressure determination procedures mentioned in Section 4.1, see Figure 4.12.

Response time test of the prototype vehicle equipped with disc brakes is conducted by using response time test procedure mentioned in Section 4.1. Response time test results are shown in Figure 4.13 below.

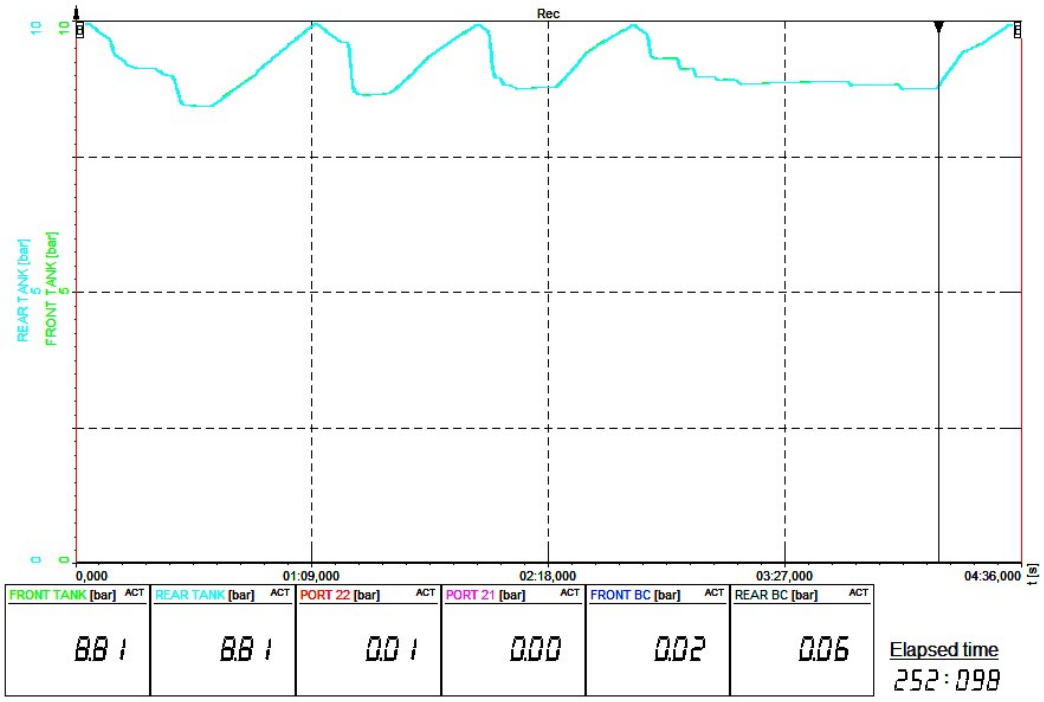

Figure 4.12 : Cut-in pressure of compressor of prototype vehicle.

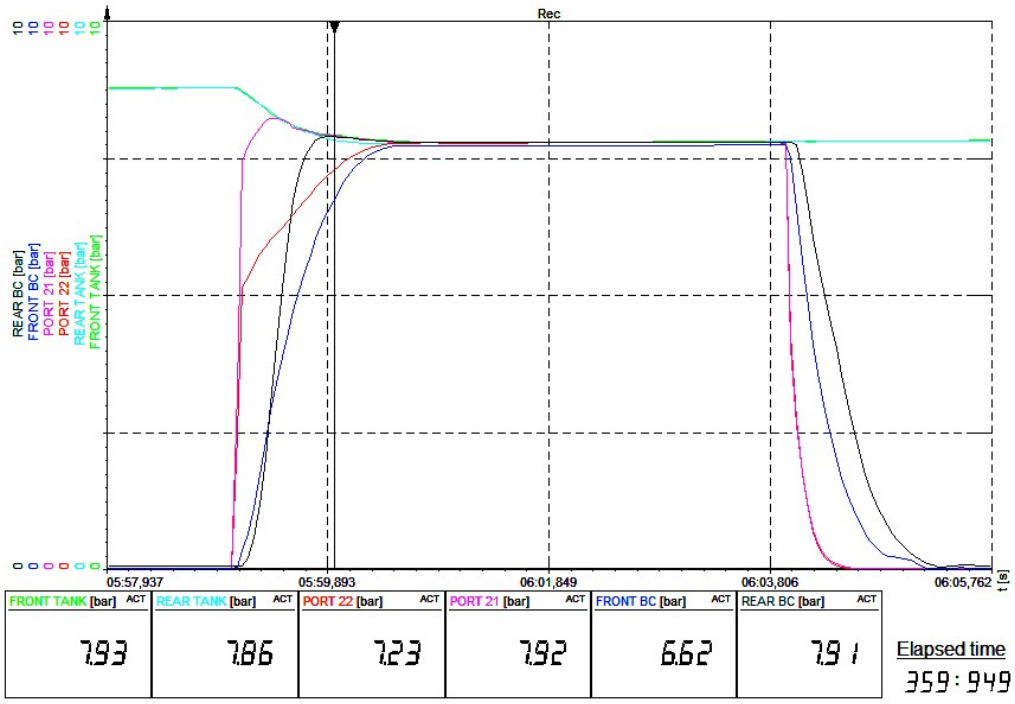

Figure 4.13 : Response time test results of prototype vehicle.

It can be seen that final pressure at the front and rear circuit deliveries of the foot brake valve is equal to 7.8 bars. Thus, the elapsed time measured from the actuation of brake pedal to the time that the pressure reaches to 10% of final pressure of the

front delivery is equal to t_{22} =0.07 s. As for the rear delivery, the elapsed time is monitored as t_{21} =0.07 s.

For the second requirement of a succeeded actuation, the elapsed time measured from the actuation of brake pedal to the time that the pressure reaches to 75% of final pressure of the front delivery is equal to t_{22} =0.3 s. As for the rear delivery, the elapsed time is monitored as t_{21} =0.1 s. It is shown that results fulfill requirements of a succeeded actuation for the response time test.

It can be calculated that 75% of the cut-in pressure of the air compressor is 6.6 bars. At this point, response time results of front and rear brake chambers are obtained as t_f =0.9 s and t_r =0.5 s respectively. Hence, it can be concluded that for the given test requirements, response time results of front circuit could not pass the test.

5. RESULTS AND DISCUSSION

In this chapter, analyses are performed by using system model, which is obtained from Chapter 3. Analysis results are verified by using experimental data taken from the vehicle tests that are done in Chapter 4. For providing system improvements, a study is conducted in which possible design alternatives are discussed on the prototype vehicle.

5.1 Analysis and Verification of the System Model

In this section, two response time analyses are conducted for the validation of the system model by using system parameters of two different heavy-duty vehicles given the details below.

5.1.1 Analysis-1: Serial Production Vehicle

5.1.1.1 System parameters of Analysis-1

In this section, analyses of the pneumatic brake system model that is constructed in Chapter 3 are performed by using system parameters of serial production vehicle, which is equipped with wedge drum brakes. Most of the system parameters are obtained from the technical datasheets of the air brake system components and from similar studies in the current literature. The other unknown system parameters will be identified in this section by using response time test of the serial production vehicle (Test-1) whose details and results are given in section 4.1. For the analysis of the serial production vehicle, defined system parameters are summarized in Table 5.1 and the details are given below.

Viscous friction coefficients (b_f, b_r and b_{rv}) and return spring constants (k_f, k_r and k_{rv}) are taken from similar studies in current literature (Kluever & Kluever, 2015; Yi et al., 2015). Maximum push–rod strokes (x_{max_f} and x_{max_r}) are taken a value of 0.027m for wedge brake with unworn linings. Other brake chamber parameters like piston/push rod masses (m_f and m_r), pre-load spring forces (F_{PL_f}

and F_{PL_r}), diaphragm cross-sectional areas (A_{b_f} and A_{b_r}), initial and maximum chamber volumes (V_{0_f}, V_{0_r},V_{max_f} and V_{max_r}) are obtained from technical drawings of front and rear brake chambers, which are showed in Appendix A.1 and A.2. For actuation purpose, two brake chambers should be mounted on a wedge brake, making in total four brake chambers for each axle. Load forces of foundation brakes (F_{load_f} and F_{load_r}) are obtained from standard brake system calculations of a 6x6 heavy-duty truck, on which same wedge brakes are used.

Discharge coefficient of foot brake valve (C_d) is taken from similar study in literature, in which the same foot brake valve is used for regulating the compressed air (Selvaraj et al., 2014). Same value is taken into consideration for discharge coefficient of relay valve (C_{d_rv}). Predominance pressure (P_{FBV}) is obtained from datasheet of foot brake valve shown in Appendix A.3.

Pre-load spring force of relay valve (F_{PL_rv}), maximum relay piston stroke ($x_{max\ \_rv}$) and cross sectional area of relay piston (A_{b_rv}) are referenced from similar studies.

It is observed from the results of Test-1 that, when the pressure at rear circuit delivery of the foot brake valve (Port 21) exceeds to its asymptotic/final value then the pressure at the rear brake chambers start increasing from zero. Therefore, the threshold pressure of relay valve (P_{th_rv}) is assumed to be equal to the steady state system pressure (P_{st}).

Pneumatic pipeline dimensions are determined according to the pneumatic service brake system layout of serial production vehicle.

Supply tank pressures are set to the value of 7.427(10^5) Pa, which is obtained from the result of Test-1, measured as compressor cut-in pressure.

Experimental pressure curves of front and rear brake chambers (P_{f_exp} and P_{r_exp}) obtained from Test-1 are introduced to the Simulink model. These experimental results are plotted together with the numerical brake chamber pressure transients (P_f and P_r). In order to identify unknown orifice cross sectional areas of FBV and RV, a series of analyses are conducted under nominal operating conditions by changing both orifice area values until the numerical pressure curves are fitted to the experimental pressure curves, see Figure 5.1. Also, actuation time of the brake pedal is set to 0.04 s for the purpose of curve fitting.

It is shown from the Simulink block in Figure 3.1 that a 1N pedal force produces a $0.015(10^{-3})$ m^2 step orifice area on the foot brake valve. This action increases the pressure at the control port of the relay valve to the threshold value of $6.586(10^5)$ Pa, producing a $0.028(10^{-3})$ m^2 step orifice area on the relay valve.

Table 5.1 : System parameters of serial production vehicle.

Supply Tank Parameters	**Symbol**	**Value**	**Unit**	**Notes**
Supply tank pressure	P_{S_f}	$7.427(10^5)$	Pa	
	P_{S_r}	$7.427(10^5)$		
Supply tank volume	V_{S_f}	$18(10^{-3})$	m^3	
	V_{S_r}	$18(10^{-3})$		
Brake Chamber Parameters	**Symbol**	**Value**	**Unit**	**Notes**
Piston/push rod mass	m_f	1.5	kg	Appendix A.1 Appendix A.2
	m_r	2		
Viscous friction coefficient	b_f	12	N-s/m	(Kluever & Kluever, 2015)
	b_r	12		
Return spring constant	k_f	1250	N/m	(Kluever & Kluever, 2015)
	k_r	1250		
Pre-load spring force	F_{PL_f}	150	N	Appendix A.1 Appendix A.2
	F_{PL_r}	150		
Diaphragm cross-sectional area	A_{b_f}	0.0774	m^2	Appendix A.1 Appendix A.2
	A_{b_r}	0.0774		
Initial push rod stroke	x_{0_f}	0	m	
	x_{0_r}	0		
Maximum push rod stroke	x_{max_f}	0.027	m	
	x_{max_r}	0.027		
Initial chamber volume $(\mathbf{x = x_0})$	V_{0_f}	$0.12(10^{-3})$	m^3	Appendix A.1 Appendix A.2
	V_{0_r}	$0.12(10^{-3})$		
Maximum chamber volume $(\mathbf{x = x_{max}})$	V_{max_f}	$0.30(10^{-3})$	m^3	Appendix A.1 Appendix A.2
	V_{max_r}	$0.30(10^{-3})$		
Initial chamber pressure $(\mathbf{x = x_0})$	P_{0_f}	0	Pa	
	P_{0_r}	0		
Number of chamber per axle	n_f	4	pcs	
	n_r	4		
Foundation Brake Parameters	**Symbol**	**Value**	**Unit**	**Notes**
Load force of foundation brake	F_{load_f}	90	N	
	F_{load_r}	90		

Table 5.1 (continued) : System parameters of serial production vehicle.

Foot Brake Valve Parameters	Symbol	Value	Unit	Notes
Driver's brake pedal force	F_{pedal}	1	N	
Orifice cross-sectional area of FBV	A_v	$0.015(10^{-3})$	m^2	
Actuating/delay time	t_{delay}	0.04	s	
Discharge coefficient of FBV	C_d	0.7	n/a	(Selvaraj et al., 2014)
Predominance pressure of FBV	P_{FBV}	$0.3039(10^5)$	Pa	Appendix A.3
Relay Valve Parameters	Symbol	Value	Unit	Notes
Relay piston mass	m_{rv}	0.1	kg	
Viscous friction coefficient of RV	b_{rv}	12	N-s/m	(Kluever & Kluever, 2015)
Return spring constant of RV	k_{rv}	1320	N/m	(Yi et al., 2015)
Pre-load spring force of RV	F_{PL_rv}	21.32	N	(Yi et al., 2015)
Initial relay piston stroke	x_{0_rv}	0	m	
Maximum relay piston stroke	x_{max_rv}	$3.5(10^{-3})$	m	(Kulesza & Siemieniako, 2010)
Initial control port pressure ($x_{rv} = x_{0\_rv}$)	P_{0_rv}	0	Pa	
Cross sectional area of relay piston	A_{b_rv}	$5.6(10^{-3})$	m^2	(Yi et al., 2015)
Orifice cross sectional area of RV	A_{v_rv}	$0.028(10^{-3})$	m^2	
Discharge coefficient of RV	C_{d_rv}	0.7	n/a	(Selvaraj et al., 2014)
Threshold pressure of RV	P_{th_rv}	$6.586(10^5)$	Pa	
Pipeline Parameters	**Symbol**	**Value**	**Unit**	**Notes**
Inner pipe diameter of Ø8x1	d_8	0.006	m	
Inner pipe diameter of Ø10x1	d_{10}	0.008	m	
Inner pipe diameter of Ø12x1.5	d_{12}	0.009	m	
Inner pipe diameter of 1/2"	d_{1_2}	0.0125	m	
Total pipe length of Ø8x1	L_8	13.183	m	
Total pipe length of Ø10x1	L_{10}	13.183	m	
Total pipe length of Ø12x1	L_{12}	5.436	m	
Total pipe length of 1/2"	L_{1_2}	1.810	m	
Other Parameters	**Symbol**	**Value**	**Unit**	**Notes**
Atmospheric pressure	P_{atm}	$1.0133(10^5)$	Pa	
Gas constant	R	287	N-m/kg-K	
Air temperature	T	298	K	
Simulation time	t_{sim}	2	s	

5.1.1.2 Results of Analysis-1

The piston/push rod response of front and rear brake chambers and relay valve to the step valve opening is shown in Figure 5.2. Brake chamber pressures (P_f and P_r) and control port pressure of relay valve (P_{rv}) are oscillating during piston/push rod travel

shown in Figure 5.3. When the push rods reach their hard stop limits (x_f=x_r=0.027m), brake chamber pressures exhibit no longer oscillatory behaviour because of the constant chamber volume ($\dot{V}_f$=$\dot{V}_r$=0). The push rods of front and rear brake chambers reach their hard stop limits (x_f=x_r=0.027m) in t_f =0.18 s and t_r =0.27 s respectively.

Mass flow rates of front and rear deliveries of FBV and relay valve are shown in Figure 5.4. When the foot brake valve and relay valve are opened, the compressed air flows chocked at w_f=0.004106 kg/s, w_{rv}=0.007665 kg/s and w_r=0.01643 kg/s until the chamber pressures exceed to P_f=P_r=P_{rv}=3.527(10^5) Pa at time t_f =0.37 s, t_r =0.37 s and t_{rv} =0.11 s. In other words, referring to equations (2.10)-(2.16), when the pressure ratio of downstream to upstream is equal to critical pressure ratio of air $C_{r=}$ 0.528, pressure values are chosen as 0.528 P_{st}. After that instant; the air flow becomes unchocked; mass flow rates of front and rear deliveries (w_f and w_r) and relay valve (w_{rv}) begin to decrease.

Brake chamber pressures (P_f, P_r) exhibit constant rate of pressure increase, when the piston/push rods have reached their hard stop limits ($\dot{V}_f$=$\dot{V}_r$=0) and mass flow rates (w_f, w_{rv}) are constant (chocked flow). This case occurs between t_{f1} =0.18 s and t_{f2} =0.38 s for front brake chamber, t_{r1} =0.27 s and t_{r2} =0.38 s for rear brake chamber respectively.

When chamber pressures (P_f, P_r and P_{rv}) reach at the steady state system pressure (P_{st}) at time t_f =0.84 s, t_r =0.62 s and t_{rv} = 0.21 s; consequently mass flow rates (w_f, w_{rv} and w_r) become zero.

75% of the cut-in pressure of the air compressor is equal to 5.5 bars. At this point, experimental and numerical response time results of front and rear brake chambers are given in Table 5.2.

When Test 1 and Analysis 1 are compared, it can be seen that the numerical pressure transients derived from Analysis 1 fit well with the results of Test-1 and they are shown in Figure 5.1. Numerical and experimental response time results obtained from serial production vehicle shows a correlation with deviations of 1.7-2% in front and rear circuits respectively (see Table 5.2), which fulfill the need of the pneumatic brake system. As mentioned in Chapter 4, legal regulation limit for response time is

given a value of 0.6 s. Hence; it is obvious that the results of Test 1 and Analysis 1 meet the needed requirements of the regulation.

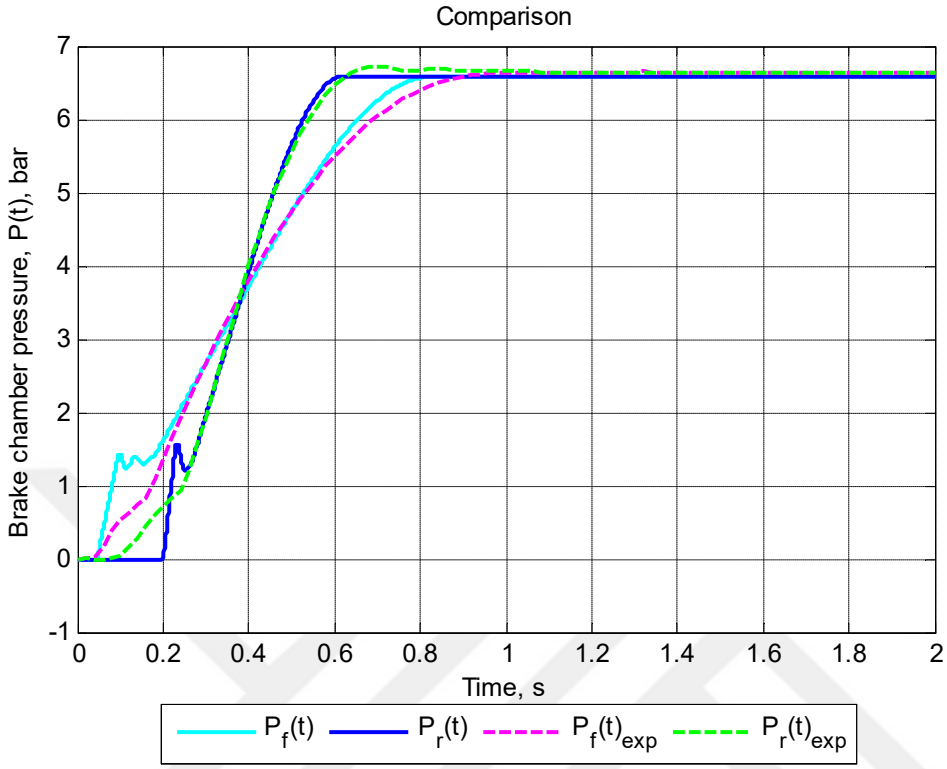

Figure 5.1 : Numerical and experimental and pressure curves.

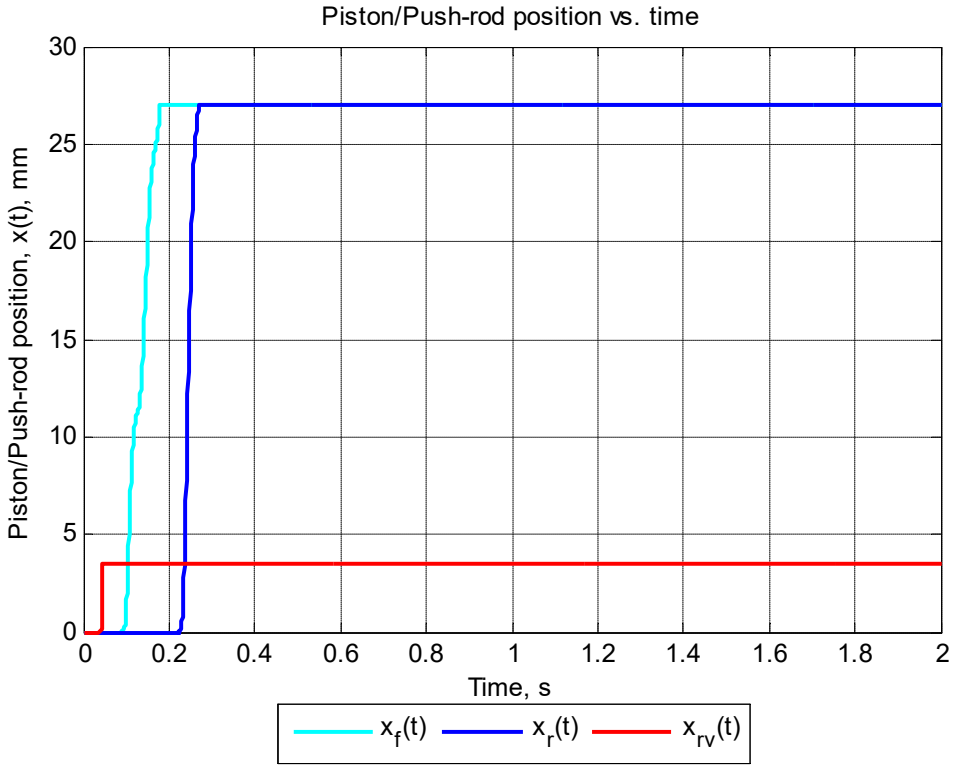

Figure 5.2 : Piston/push rod position vs. time.

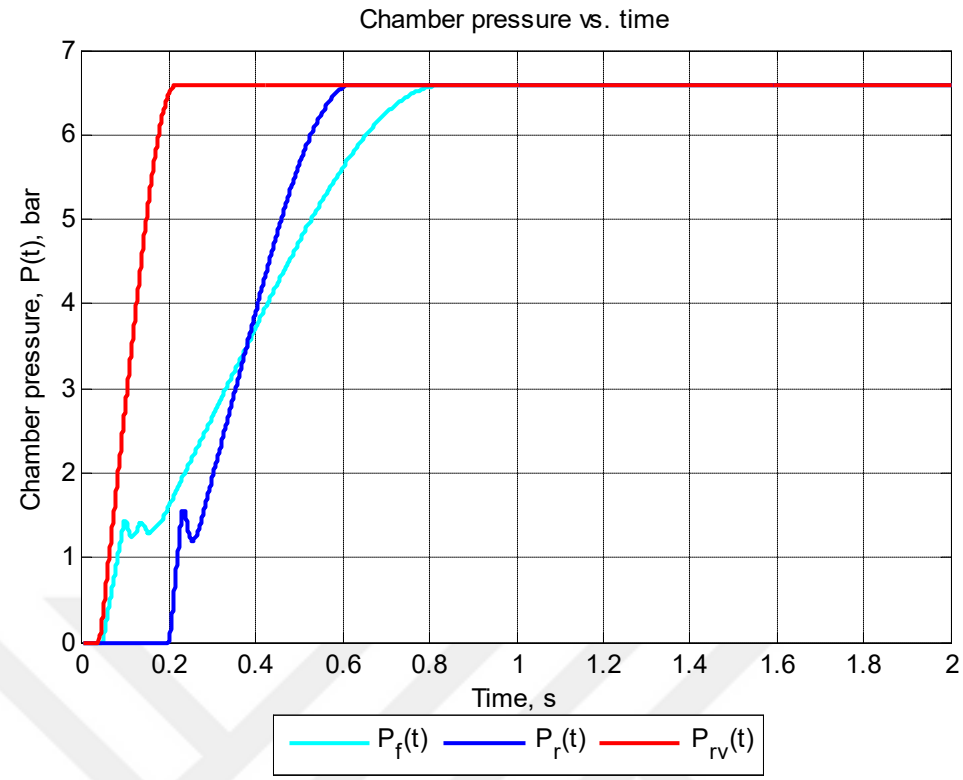

Figure 5.3 : Chamber pressure vs. time.

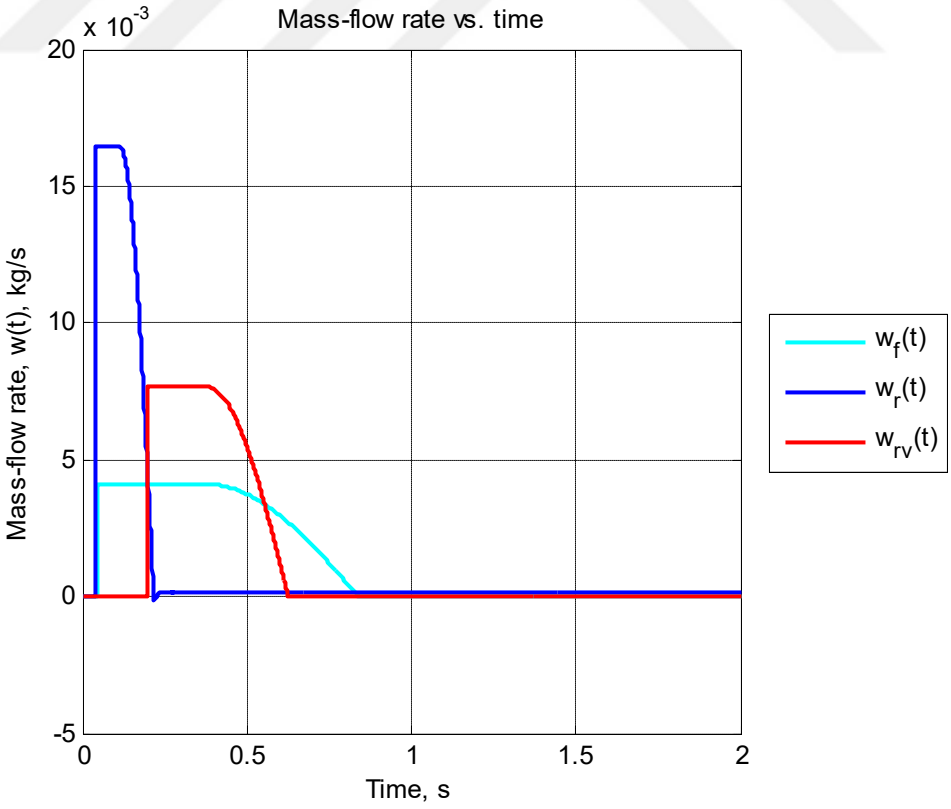

Figure 5.4 : Mass flow rate vs. time.

Table 5.2 : Numerical and experimental response time results.

	Numerical results (s)	Experimental results (s)	Error (%)
Front circuit	0.59	0.58	1.7 %
Rear circuit	0.49	0.48	2 %

5.1.2 Analysis-2: Prototype Vehicle

5.1.2.1 System parameters of Analysis-2

For the validation of the pneumatic brake system model, Analysis-2 is conducted by using system parameters of prototype vehicle whose response time measurements (Test-2) are performed in section 4.2. The vehicle is equipped with the disc brakes. The predicted numerical results are compared with Test-2 results. The system parameters used in the analysis of the prototype vehicle are tabulated in Table 5.3 and the details are given below.

The pneumatic valves that are used in the serial production vehicle are also used in the pneumatic brake system of the prototype vehicle therefore; same FBV and RV parameters are taken into consideration for analyses of the prototype vehicle.

Supply tank pressures are defined to be equal to the compressor cut-in pressure measured in Test-2, which is 8.917(10^5) Pa. Threshold pressure of relay valve (P_{th_rv}) is equal to steady state system pressure (P_{st}) a value of 7.802(10^5) Pa.

Disc brake application is implemented on the prototype vehicle. Hence, two disc brake chambers are mounted on each axle. Load forces of foundation brakes (F_{load_f} and F_{load_r}) are obtained from technical drawing of the disc brake. Maximum push rod strokes of disc brake chambers ($x_{max\ \_f}$ and $x_{max\ \_r}$) are taken a value of 0.036 m for unworn linings. Other brake chamber parameters are obtained from technical drawings of the front and rear brake chambers.

Approximate pipeline dimensions of prototype vehicle shown in Table 5.3 are introduced into the pneumatic brake system model.

Table 5.3 : System parameters of prototype vehicle.

Supply Tank Parameters	Symbol	Value	Unit	Notes
Supply tank pressure	P_{S_f}	$8.917(10^5)$	Pa	
	P_{S_r}	$8.917(10^5)$		
Supply tank volume	V_{S_f}	$18(10^{-3})$	m^3	
	V_{S_r}	$18(10^{-3})$		
Brake Chamber Parameters	**Symbol**	**Value**	**Unit**	**Notes**
Piston/push rod mass	m_f	2	kg	Appendix A.4 Appendix A.5
	m_r	4		
Viscous friction coefficient	b_f	12	N-s/m	(Kluever & Kluever, 2015)
	b_r	12		
Return spring constant	k_f	1250	N/m	(Kluever & Kluever, 2015)
	k_r	1250		
Pre-load spring force	F_{PL_f}	200	N	Appendix A.4 Appendix A.5
	F_{PL_r}	220		
Diaphragm cross-sectional area	A_{b_f}	0.0155	m^2	Appendix A.4 Appendix A.5
	A_{b_r}	0.0129		
Initial push rod stroke	x_{0_f}	0	m	
	x_{0_r}	0		
Maximum push rod stroke	x_{max_f}	0.036	m	
	x_{max_r}	0.036		
Initial chamber volume $(\mathbf{x = x_0})$	V_{0_f}	$0.27(10^{-3})$	m^3	Appendix A.4 Appendix A.5
	V_{0_r}	$0.20(10^{-3})$		
Maximum chamber volume $(\mathbf{x = x_{max}})$	V_{max_f}	$0.75(10^{-3})$	m^3	Appendix A.4 Appendix A.5
	V_{max_r}	$0.70(10^{-3})$		
Initial chamber pressure $(\mathbf{x = x_0})$	P_{0_f}	0	Pa	
	P_{0_r}	0		
Number of chamber per axle	n_f	2	pcs	
	n_r	2		
Foundation Brake Parameters	**Symbol**	**Value**	**Unit**	**Notes**
Load force of foundation brake	F_{load_f}	90	N	Appendix A.6
	F_{load_r}	90		
Foot Brake Valve Parameters	**Symbol**	**Value**	**Unit**	**Notes**
Driver's brake pedal force	F_{pedal}	1	N	
Orifice cross-sectional area of FBV	A_v	$0.015(10^{-3})$	m^2	
Actuating/delay time	t_{delay}	0.04	s	
Discharge coefficient of FBV	C_d	0.7	n/a	(Selvaraj et al., 2014)
Predominance pressure of FBV	P_{FBV}	$0.3039(10^5)$	Pa	Appendix A.3

Table 5.3 (continued) : System parameters of prototype vehicle.

Relay Valve Parameters	Symbol	Value	Unit	Notes
Relay piston mass	m_{rv}	0.1	kg	
Viscous friction coefficient of RV	b_{rv}	12	N-s/m	(Kluever & Kluever, 2015)
Return spring constant of RV	k_{rv}	1320	N/m	(Yi et al., 2015)
Pre-load spring force of RV	F_{PL_rv}	21.32	N	(Yi et al., 2015)
Initial relay piston stroke	x_{0_rv}	0	m	
Maximum relay piston stroke	x_{max_rv}	$3.5(10^{-3})$	m	(Kulesza & Siemieniako, 2010)
Initial control port pressure ($x_{rv} = x_{0\_rv}$)	P_{0_rv}	0	Pa	
Cross sectional area of relay piston	A_{b_rv}	$5.6(10^{-3})$	m^2	(Yi et al., 2015)
Orifice cross sectional area of RV	A_{v_rv}	$0.028(10^{-3})$	m^2	
Discharge coefficient of RV	C_{d_rv}	0.7	n/a	(Selvaraj et al., 2014)
Threshold pressure of RV	P_{th_rv}	$7.802(10^5)$	Pa	
Pipeline Parameters	**Symbol**	**Value**	**Unit**	**Notes**
Inner pipe diameter of Ø8x1	d_8	0.006	m	
Inner pipe diameter of Ø10x1	d_{10}	0.008	m	
Inner pipe diameter of Ø12x1.5	d_{12}	0.009	m	
Inner pipe diameter of 1/2"	d_{1_2}	0.0125	m	
Total pipe length of Ø8x1	L_8	13.183	m	
Total pipe length of Ø10x1	L_{10}	0	m	
Total pipe length of Ø12x1	L_{12}	11.831	m	
Total pipe length of 1/2"	L_{1_2}	5.530	m	
Other Parameters	**Symbol**	**Value**	**Unit**	**Notes**
Atmospheric pressure	P_{atm}	$1.0133(10^5)$	Pa	
Gas constant	R	287	N-m/kg-K	
Air temperature	T	298	K	
Simulation time	t_{sim}	2	s	

5.1.2.2 Results of Analysis-2

Experimental pressure curves of front and rear brake chambers (P_{f_exp} and P_{r_exp}) obtained from Test-2 are introduced to the Simulink model. These experimental results are plotted together with the numerical brake chamber pressure transients (P_f and P_r), see in Figure 5.5.

75% of the cut-in pressure of the air compressor is equal to 6.6 bars. At this point, experimental and numerical response time results of front and rear brake chambers are given in Table 5.4.

When Test 2 and Analysis 2 results are compared; it can be shown in Figure 5.5 that the tendencies of the numerical and experimental pressure transients are similar and there is only a little difference in front circuit results. As shown in Table 5.4,

deviations between numerical and experimental results of front and rear circuits are 12.9% and 3.8% respectively for the prototype vehicle equipped with disc brakes.

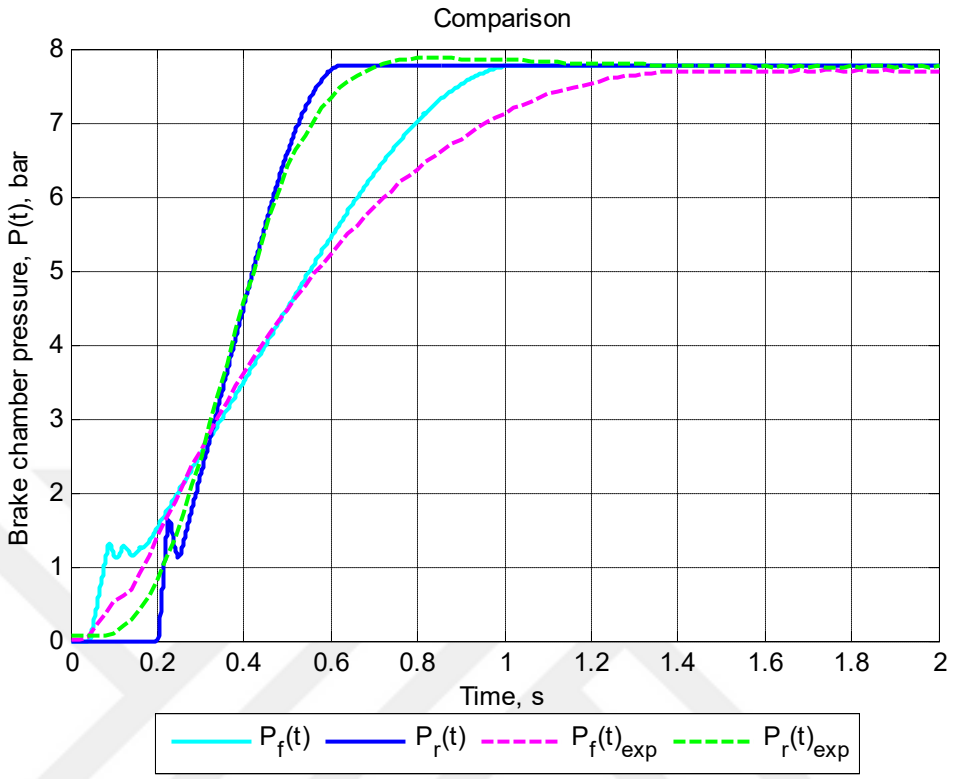

Figure 5.5 : Numerical and experimental pressure curves of prototype vehicle.

Table 5.4 : Numerical and experimental response time results of prototype vehicle.

	Numerical results (s)	Experimental results (s)	Error (%)
Front circuit	0.74	0.85	12.9 %
Rear circuit	0.50	0.52	3.8 %

Deviations and errors between Test 2 and Analysis 2 may occur due to the following reasons;

• Test 2 and Analysis 2 are conducted on the prototype vehicle. Because of the limitations in the measurement of pneumatic pipeline, exact pipe lengths could not be determined accordingly. For this reason, approximate pipe lengths are introduced into the Simulink model for the analyses. Test 1 is performed on the serial production vehicle therefore; pipeline dimensions, which are taken for Analysis 1, are obtained from the pneumatic layout and technical drawings of pipes and tubes used in pneumatic brake system.

• In analyses, push rod stroke values of front and rear brake chambers are taken as if the foundation brakes have unworn linings. Analysis 1 is performed on the serial production vehicle whose response time test is conducted immediately after the

production and has very new linings. On the other side, for the prototype vehicle, on which Test-2 is conducted, linings are mounted on the calipers could be worn.

• Pressure losses due to the friction in the pipeline used in pneumatic brake system are not taken into consideration in the mathematical system model.

Although maximum deviation between Test 2 and Analysis 2 of the front circuit is obtained as 12.9%, this deviation corresponds to a value of 0.11 s only. Beside, it can be observed that the numerical pressure data can follow the behavior of the experimental curves, as shown in Figure 5.5. Hence, this correlation is assumed to be enough and acceptable for response time prediction of the pneumatic brake system.

In addition, it can be shown from the numerical and experimental response time results that rear circuit fulfills the legal regulation limit of 0.6 s. Unlikely; front circuit does not meet the requirements of the regulation.

5.2 System Improvements

In order to provide system improvements, a study whose details can be seen below is done, in which possible design alternatives are discussed on the prototype vehicle. For this purpose, response time of front circuit is tried to be improved by making some design modifications on the pneumatic brake system properties like supply tank capacities, brake chamber size and related brake chamber parameters (i.e. diaphragm cross sectional area, initial and maximum chamber volumes).

Five different analyses are performed on the prototype vehicle for each design modification, as shown in Table 5.5 below. Response time result of rear circuit fulfills the legal requirements therefore; rear brake chamber size and its parameters are kept fixed in all design points. In the first design point (DP1), supply tank volumes are increased from 18 to 30 liters, front brake chamber type and parameters are not changed. Because of the packaging issues, both supply tanks capacities are increased by taking into consideration that the pneumatic brake system permits shared volume consumption of front and rear tanks until front and rear supply tank pressures reach at the closing pressure of the quadruple protection valve. In the second design point (DP2), front brake chamber size is decreased from Type 24 to Type 22 and supply tank volumes are kept as 18 liters. As for the third design point (DP3), supply tank volumes are set to 30 liters and Type 22 brake chamber is selected. In the fourth design point (DP4), supply tank volumes are kept as 18 liters

and brake chamber size is decreased to Type 20. In the last design point (DP5), front brake chamber size is selected as Type 20 and supply tank volumes are equal to 30 liters.

Table 5.5 : Design modifications on the pneumatic brake system properties.

	Symbol	Unit	Current design (CD)	DP1	DP2	DP3	DP4	DP5
Supply tank volume	V_{S_f}	m^3	$18(10^{-3})$	$30(10^{-3})$	$18(10^{-3})$	$30(10^{-3})$	$18(10^{-3})$	$30(10^{-3})$
	V_{S_r}		$18(10^{-3})$	$30(10^{-3})$	$18(10^{-3})$	$30(10^{-3})$	$18(10^{-3})$	$30(10^{-3})$
Diaphragm area	A_{b_f}	m^2	0.0155	0.0155	0.0142	0.0142	0.0129	0.0129
	A_{b_r}		0.0129	0.0129	0.0129	0.0129	0.0129	0.0129
Initial chamber volume	V_{0_f}	m^3	$0.27(10^{-3})$	$0.27(10^{-3})$	$0.25(10^{-3})$	$0.25(10^{-3})$	$0.20(10^{-3})$	$0.20(10^{-3})$
	V_{0_r}		$0.20(10^{-3})$	$0.20(10^{-3})$	$0.20(10^{-3})$	$0.20(10^{-3})$	$0.20(10^{-3})$	$0.20(10^{-3})$
Maximum chamber volume	V_{max_f}	m^3	$0.75(10^{-3})$	$0.75(10^{-3})$	$0.78\ (10^{-3})$	$0.78(10^{-3})$	$0.70(10^{-3})$	$0.70(10^{-3})$
	V_{max_r}		$0.70(10^{-3})$	$0.70(10^{-3})$	$0.70(10^{-3})$	$0.70(10^{-3})$	$0.70(10^{-3})$	$0.70(10^{-3})$

The first thing to conclude about the modifications on the pneumatic brake system properties (Table 5.5) is that changing brake chamber size and supply tank capacities directly affect the response time. Those effects are tabulated in Table 5.6.

When looking at first design point (DP1), it can be seen that the increase in supply tank capacities decreases the response time of front and rear circuits 0.70 and 0.46 s respectively. The second design point (DP2) shows that the decrease in size of front brake chamber provide enhancement only in response time of front circuit by a percentage of 8.1. Although front brake chamber size is decreased to Type 22 and supply tank capacities are increased to 18 liters in the third design point (DP3), this modification is not sufficient since response time of front circuit reaches a value of 0.65 s with an enhancement of 12.1%. As can be seen in the fourth and the fifth design points (DP4 and DP5) the needed requirements of the regulation fulfill with response time of 0.60 and 0.57 s; in other words with enhancements of 18.9% and 22.9% respectively. Pressure transients of front and rear brake chambers are given in Figures 5.6-5.10 for each design point.

It can also be concluded that the regulation limit is fulfilled by making related modifications that are decrease in size of front brake chamber to Type 20 and increase in supply tank capacities to 30 liters in DP5 therefore, vehicle dynamics of brake calculations and charging time of the compressor should be considered.

Table 5.6 : Response time results from the different design modification analyses.

	Current design (CD)	DP1	DP2	DP3	DP4	DP5
Front circuit	0.74s	0.70s (5.7%)	0.68s (8.1%)	0.65s (12.1%)	0.60s (18.9%)	0.57s (22.9%)
Rear circuit	0.50s	0.46s (8.0%)	0.50s (0%)	0.46s (8.0%)	0.50s (0%)	0.46s (8.0%)

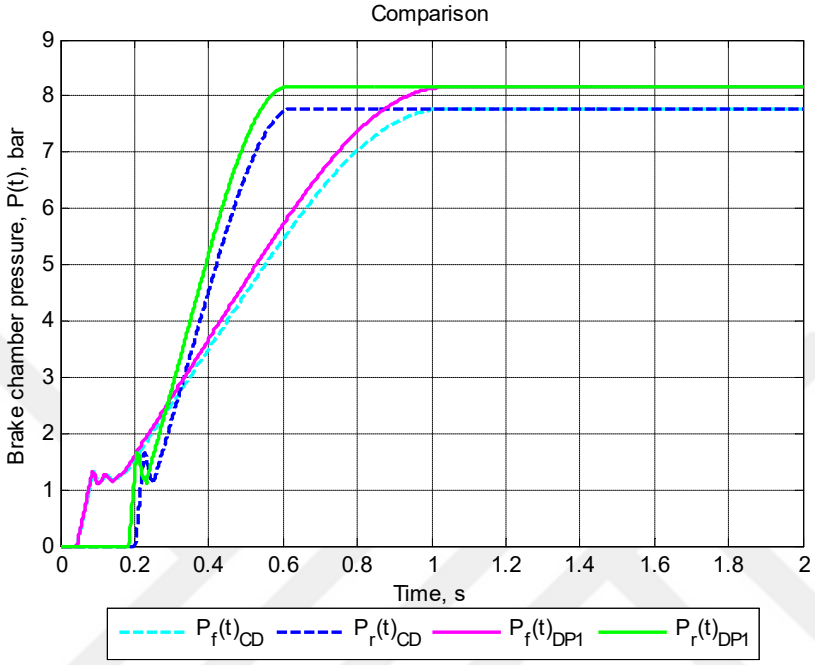

Figure 5.6 : Pressure transients of DP1.

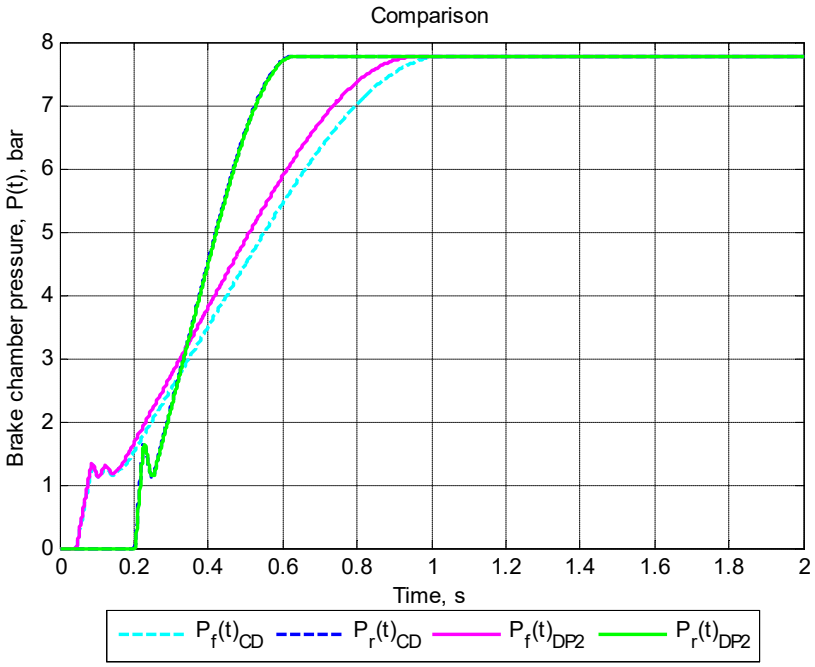

Figure 5.7 : Pressure transients of DP2.

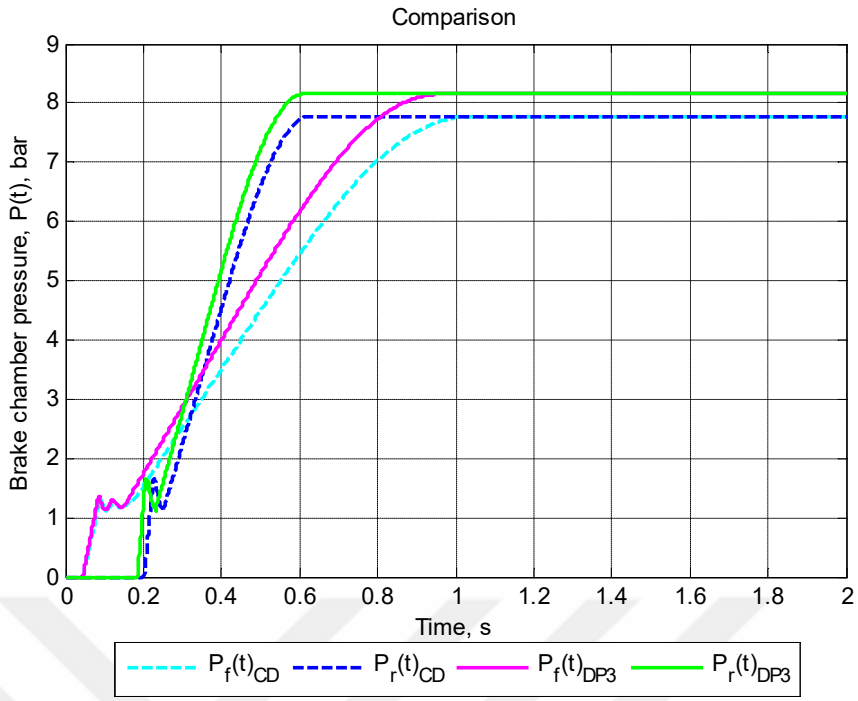

Figure 5.8 : Pressure transients of DP3.

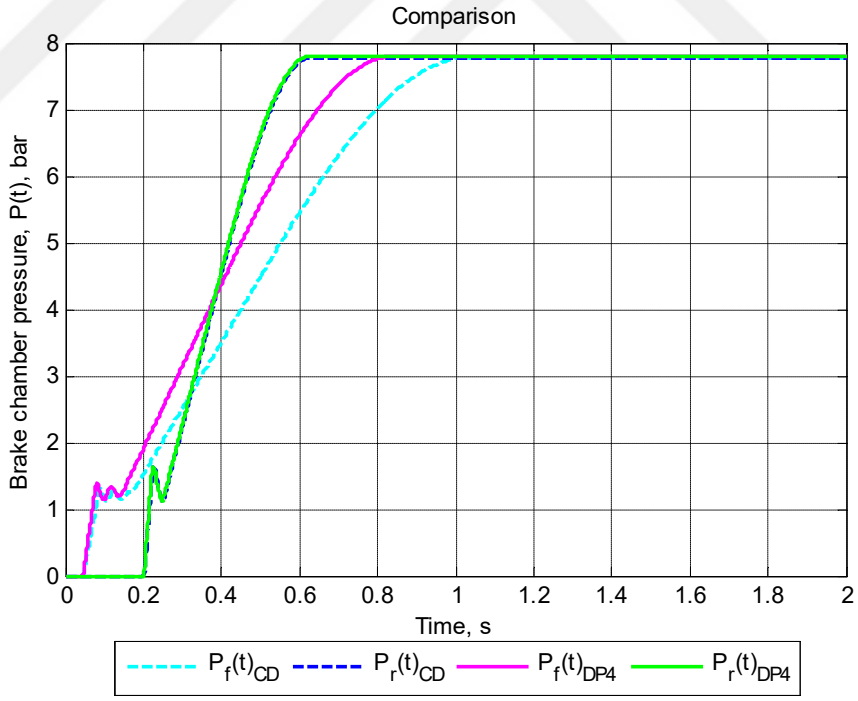

Figure 5.9 : Pressure transients of DP4.

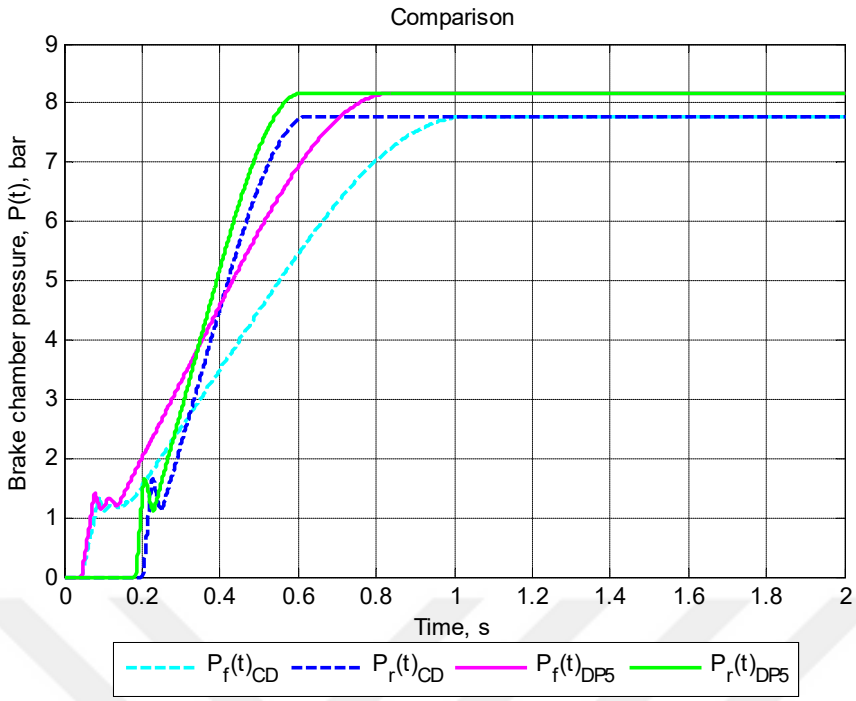

Figure 5.10 : Pressure transients of DP5.

6. CONCLUSION

As the technology develops, the development in vehicle safety becomes an area, which takes the attraction of the researchers who are working in automotive industry. Although systems like air bag system, lane departure warning system (LDWS) and tire pressure monitoring system (TPMS) improve the safety of the vehicle, main studies, in which advanced technology is used mostly focus on the brake system including anti-lock braking system (ABS), traction control system (TCS), electronic stability control (ESC), advanced emergency braking system (AEBS), adaptive cruise control (ACC). Thus, detailed studies should be conducted on brake and brake system mechanism to understand, which parameters affect the braking performance of the vehicle.

In this study, a general mathematical model is proposed to determine the dynamic characteristics of pneumatic brake system. For this purpose, first of all the details of pneumatic and mechanical subsystems of the air brake system are investigated. After that in order to be able to execute the simulations, mathematical equations of the mechanical and pneumatic subsystems are derived and these equations adapted to the Simulink model.

When constructing the Simulink model, some system parameters are obtained from the basic models in the literature and some are taken from the technical datasheets of the brake system components. Since a more complicated pneumatic brake system is aimed to be modeled, much more system parameters are required to be estimated. To identify those unknown parameters, response time tests (Test 1) are performed on a heavy-duty vehicle equipped with wedge drum brakes. The experimental results of those tests are used to tune the system model (Analysis 1) for the unknown parameters.

For verification, simulations (Analysis 2), which include proposed pneumatic brake system model should be performed on a different vehicle and these numerical results should be verified with the vehicle tests. Here a prototype heavy-duty vehicle equipped with disc brakes is used for the experimental study (Test 2).

For providing system improvements, a study is done, in which possible design alternatives are discussed on the prototype vehicle. In this study, response time of front circuit is tried to be improved by making some design modifications on the pneumatic brake system properties, therefore five different analyses are performed on the prototype vehicle and their effects are discussed.

As the final outcome of the study, when the simulation results are compared with the experimental data taken from vehicle tests, it can be seen that the pneumatic brake system model is able to predict the response time accurately. Hence, developed system model can be used as a modal based design tool for the determination of the dynamic characteristics of the pneumatic brake system during the design phase of a new brake system.

REFERENCES

Brubaker, C. L. (2015). *Dynamic Model of a Non-Linear Pneumatic Pressure Modulating Valve Using Bond Graphs* (Doctoral dissertation, Cleveland State University).

Day, A. J. (2014). *Braking of road vehicles*. Butterworth-Heinemann.

He, L., Wang, X., Zhang, Y., Wu, J., & Chen, L. (2011, June). Modeling and simulation vehicle air brake system. In *Proceedings of the 8th International Modelica Conference; March 20th-22nd; Technical Univeristy; Dresden; Germany* (No. 063, pp. 430-435). Linköping University Electronic Press.

Kluever, R. C., & Kluever, C. A. (2015). *Dynamic Systems: Modeling, Simulation, and Control*. John Wiley & Sons.

Kulesza, Z., & Siemieniako, F. (2010). Modeling the air brake system equipped with the brake and relay valves. *Zeszyty Naukowe/Akademia Morska w Szczecinie*, 5-11.

Limpert, R. (1992). *Brake design and safety* (Vol. 120).

Ramaratham, S. (2008). *A mathematical model for air brake systems in the presence of leaks* (Doctoral dissertation, Texas A&M University).

Selvaraj, M.,Mariappa, S., Gayakwad, S. (2014). Modeling and simulation of pneumatic brake system used in heavy commercial vehicle. *IOSR Journal of Mechanical and Civil Engineering*, *11*(1), 1-9.

Selvaraj, M., Gaikwad, S., & Suresh, A. K. (2014). *Modeling and Simulation of Dynamic Behavior of Pneumatic Brake System at Vehicle Level* (No. 2014-01-2494). SAE Technical Paper.

Subramanian, S. C., Darbha, S., &Rajagopal, K. R. (2003). Modeling the pneumatic subsystem of an S-cam air brake system. *Master's thesis, Texas A&M University, Faculty of Mechanical Engineering.*

Subramanian, S. C., Darbha, S., & Rajagopal, K. R. (2006). A diagnostic system for air brakes in commercial vehicles. *IEEE Transactions on Intelligent Transportation Systems*, *7*(3), 360-376.

UN, (2014). UNECE Regulation 13. Uniform provisions concerning the approval of vehicles of categories M, N and O with regard to braking, E/ECE/324/Rev.1/Add.12/Rev.8, March 2014.

Yi, L., Bowen, X., & Bin, G. (2015). Dynamic Modeling and Experimental Verification of Bus Pneumatic Brake System. *Open Mechanical Engineering Journal*, *9*, 52-57.

APPENDICES

APPENDIX A: Technical datasheets of pneumatic brake system components

APPENDIX B: M-files

APPENDIX A

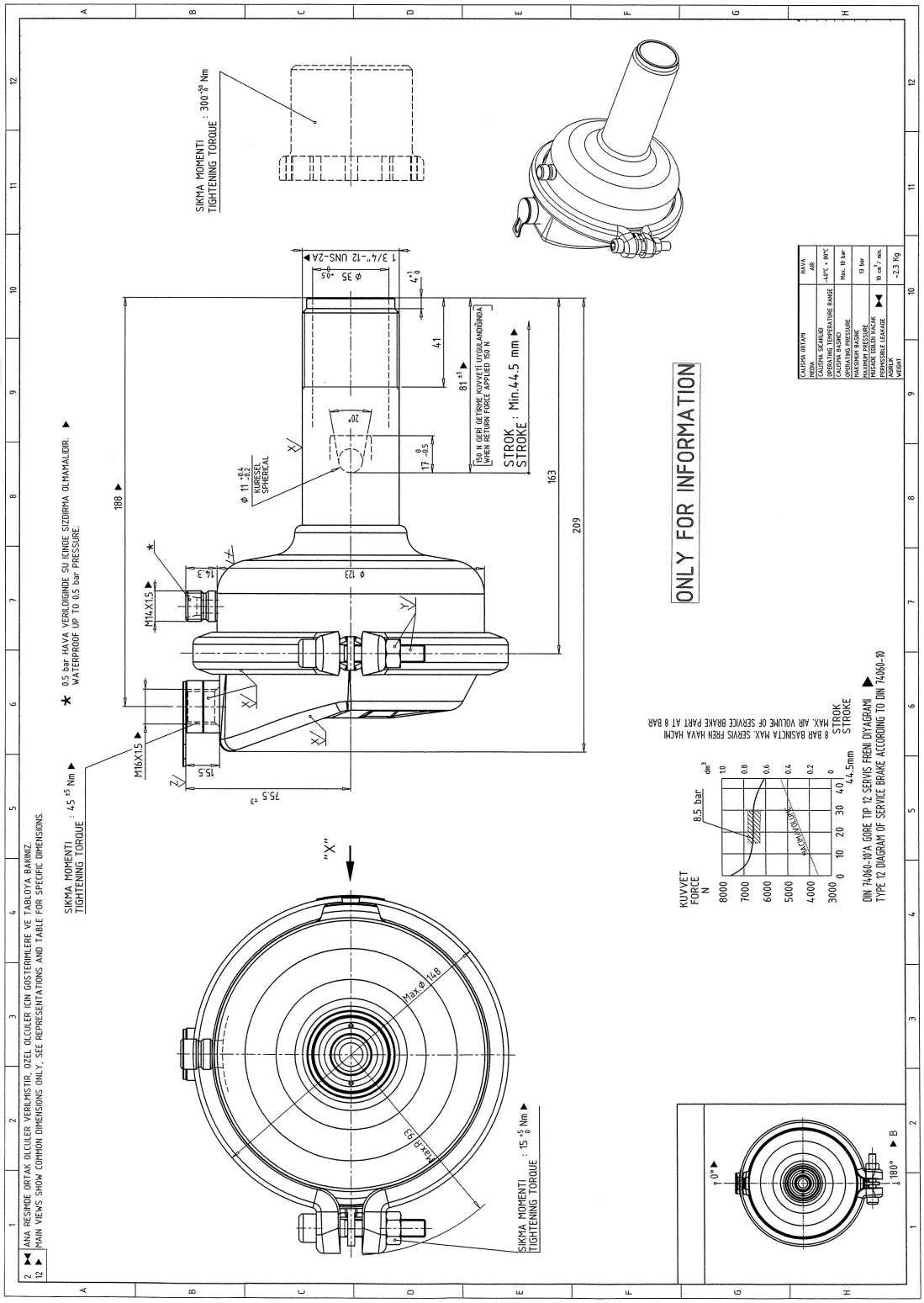

Figure A.1 : Technical drawing of service brake chamber-wedge.

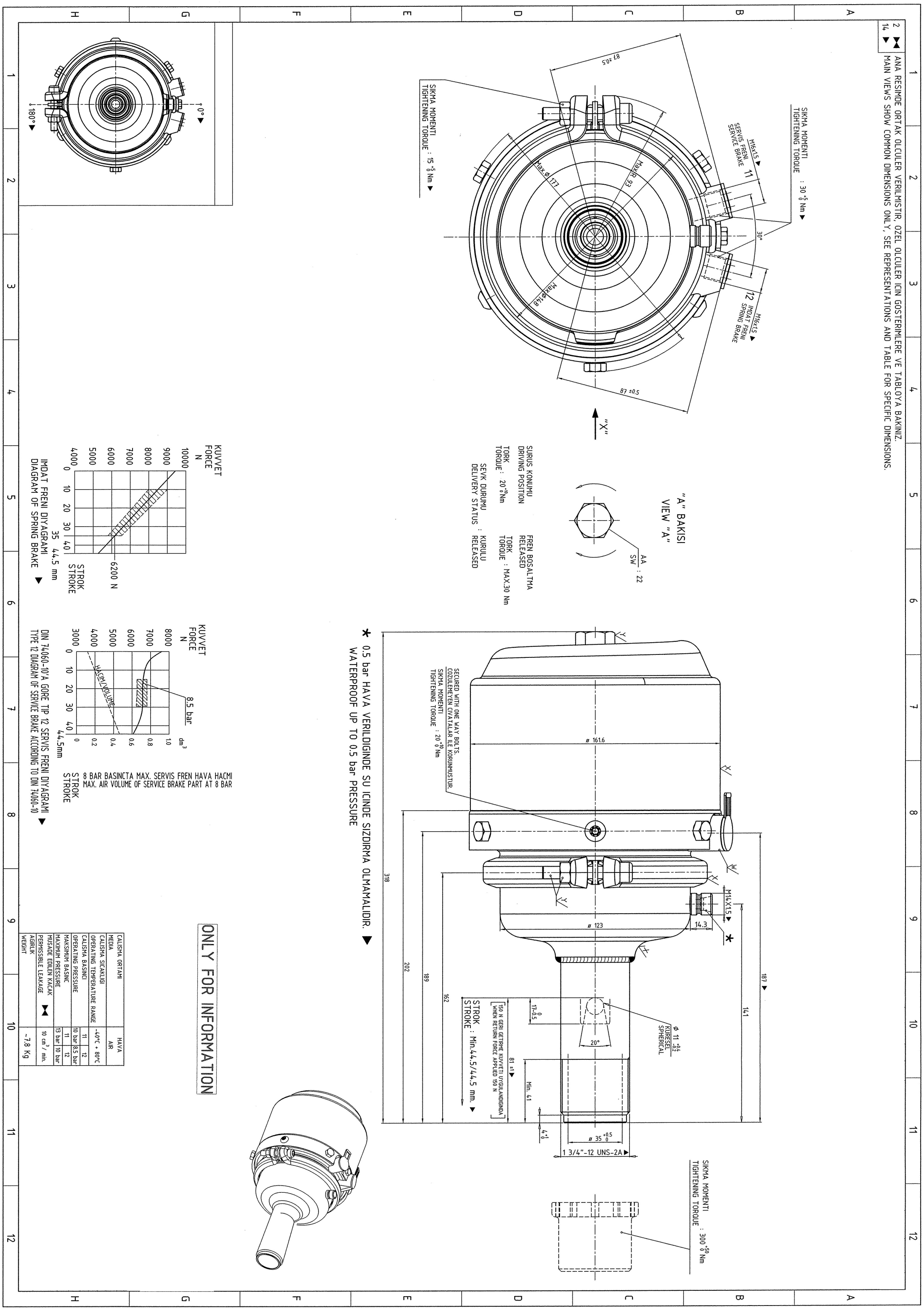

Figure A.2 : Technical drawing of spring brake chamber-wedge.

Válvula de freno
Brake Valve

Instalación / Installation:

Tipo / Type C

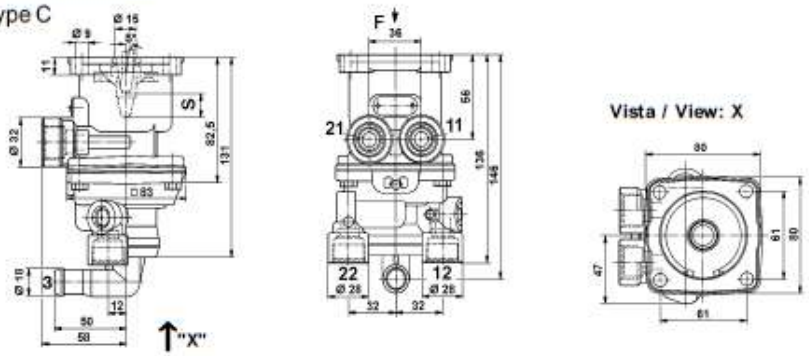

Posición de las bocas Position of ports	Tipo Type	Rec. del émbolo Way of plunger	Predominio Predominance Δ ρ	Bocas Ports	Observaciones Comments
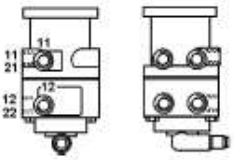	A	15,1	0,3	4x M 16x1,5 2x M 12x1,5	
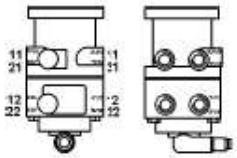	A	15,1	0,3	8x M 16x1,5	
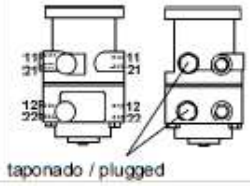 taponado / plugged	A	14	0,3	8x M 16x1,5	Bocas 11,12 con filtro Bocas 21,22 abiertas y roscadas; Port 11,12 with strainer Port 21,22 one each plugged
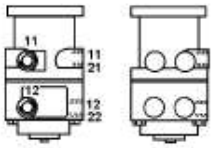	A	14	0	4x M 16x1,5 2x M 12x1,5	Bocas 11,12 con filtro Bocas 21,22 abiertas y roscadas; Port 11,12 with strainer Port 21,22 one each plugged
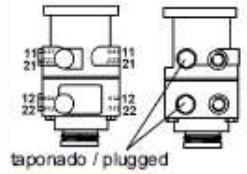 taponado / plugged	A	14	0	8x M 16x1,5	Bocas 11,12 con filtro Port 11,12 with strainer

Figure A.3 : Technical datasheet of foot brake valve.

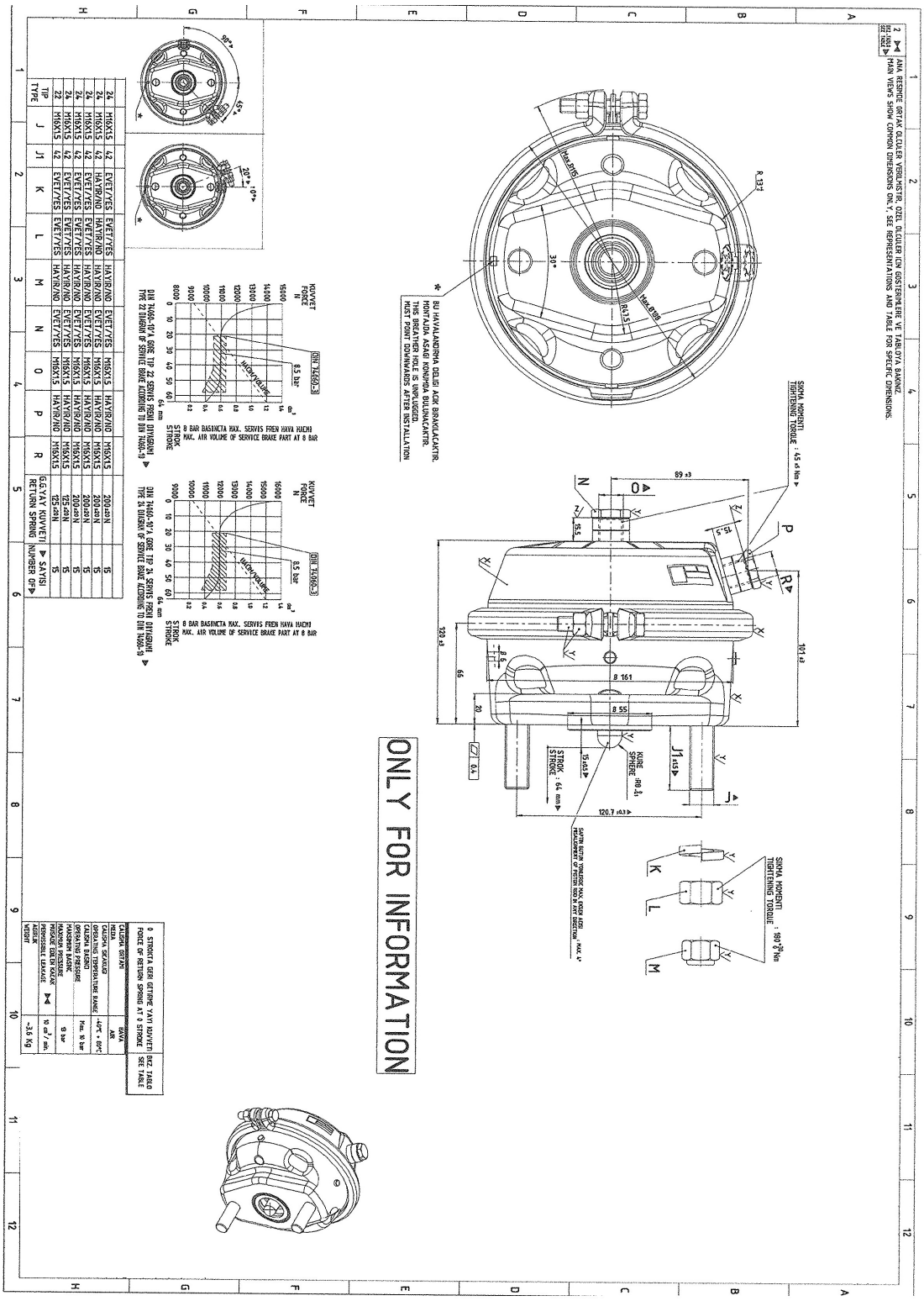

Figure A.4 : Technical drawing of service brake chamber-disc.

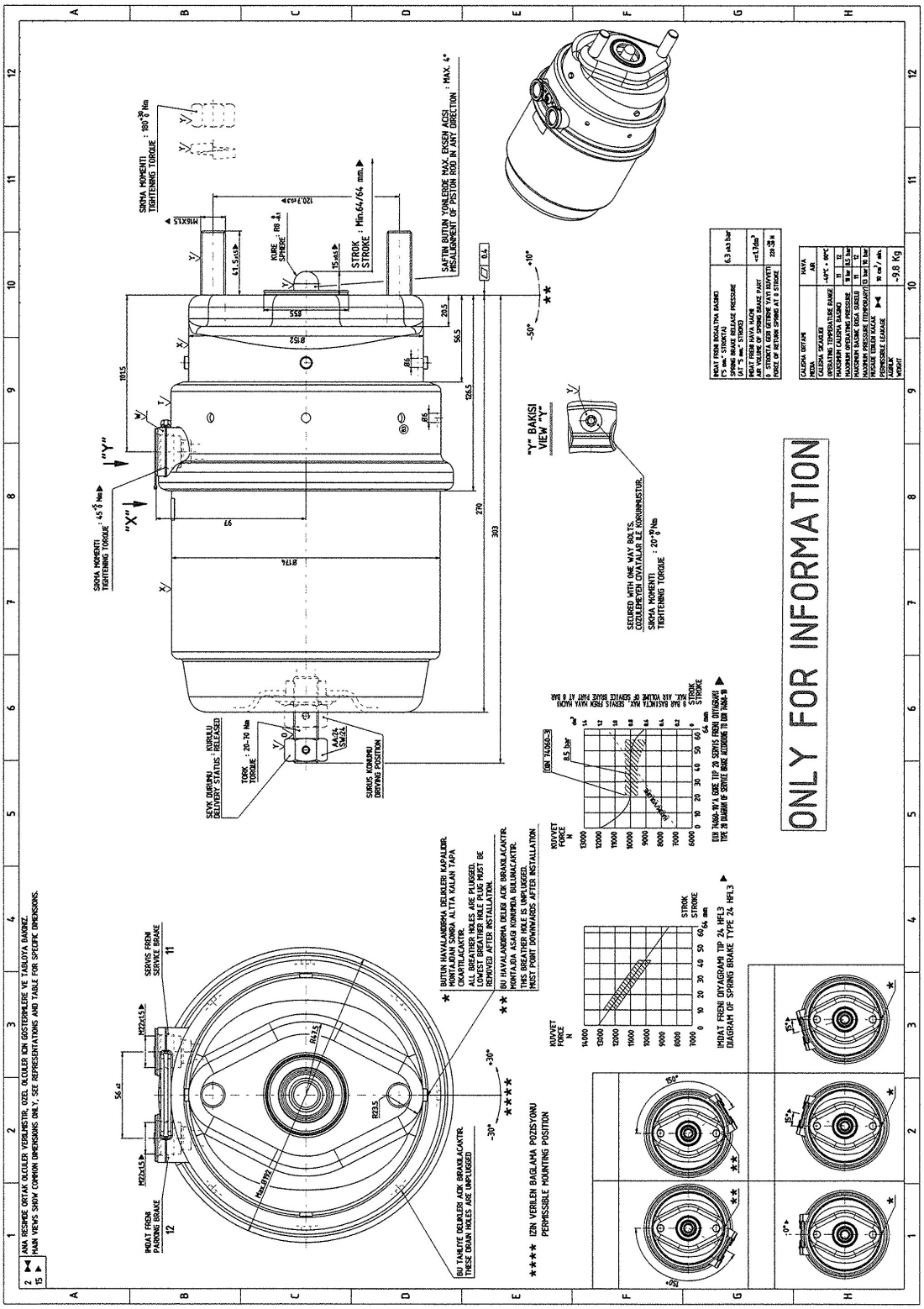

Figure A.5 : Technical drawing spring brake chamber-disc.

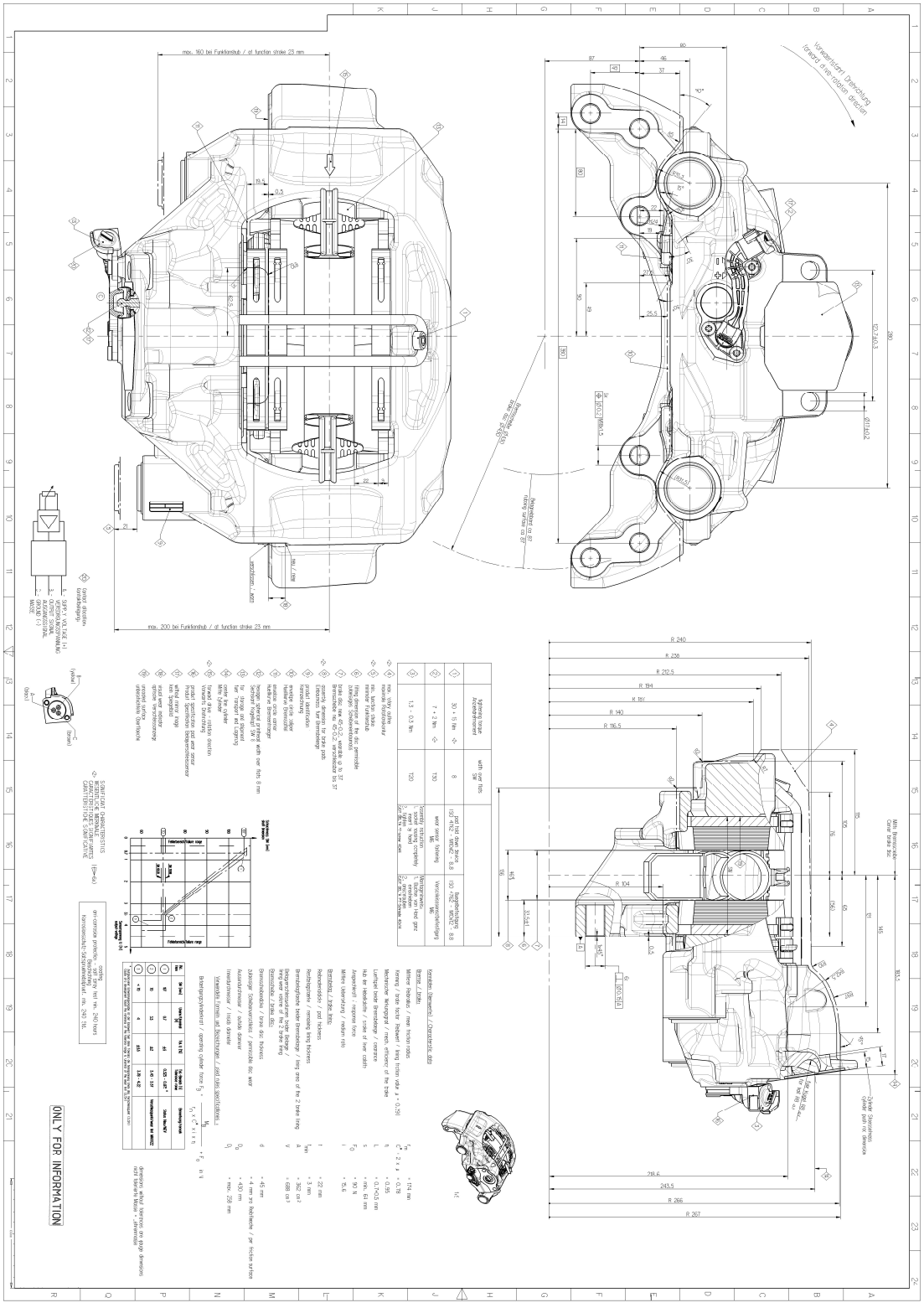

Figure A.6 : Technical drawing of disc brake.

APPENDIX B

```
%
%   run_air_brake.m
%
%   This M-file sets the modeling parameters for the
%   pneumatic air-brake system, executes the Simulink model,
%   and plots the dynamic variables

clc;clear all;

% Supply tank pressures
P_atm = 1.0133e5;              %  ambient (atmospheric) pressure, Pa
P_s_f = 7.33*P_atm;            %  supply tank pressure-front, Pa
P_s_r = P_s_f;                 %  supply tank pressure-rear, Pa
V_s_f = 18e-3;                 %  supply tank volume-front, m^3
V_s_r = 18e-3;                 %  supply tank volume-rear, m^3

%  Brake chamber parameters
Ab_f = 0.00774;                %  area of diaphragm-front, m^2
Ab_r = 0.00774;                %  area of diaphragm-rear, m^2

m_f = 1.5;                     %  diaphragm + rod mass-front brake chamber, kg
m_r = 2;                       %  diaphragm + rod mass-rear brake chamber, kg

b_f = 12;                      %  viscous friction coefficient-front, N-s/m
b_r = 12;                      %  viscous friction coefficient-rear, N-s/m

k_f = 1250;                    %  return spring constant-front, N/m
k_r = 1250;                    %  return spring constant-rear, N/m

F_PL_f= 150;                   %  return spring pre-load-front, N
F_PL_r= 150;                   %  return spring pre-load-rear, N

x0_f = 0;                      %  initial position of diaphragm-front, m
x0_r = x0_f;                   %  initial position of diaphragm-rear, m

x_max_f = 0.027;               %  max displacement of push-rod-front, m
x_max_r = x_max_f;             %  max displacement of push-rod-rear, m

P0_f = 0*P_atm;                %  initial pressure in brake chamber-front, Pa
P0_r = 0*P_atm;                %  initial pressure in brake chamber-rear, Pa

V_max_f = 0.30e-3;             %  air chamber volume @ x_max-front, m^3
V_max_r = 0.30e-3;             %  air chamber volume @ x_max-rear, m^3

n_f=4;                         %  brake chamber number @ front axle
n_r=4;                         %  brake chamber number @ rear axle

%  Foundation brake parameters
F_load_f = 90;                 %  foundation brake load force-front brake, N
F_load_r = F_load_f;           %  foundation brake load force-rear brake, N

%  Foot brake valve parameters
F_pedal = 1;                   %  unit pedal force, N
Av=15e-6;                      %  valve orifice area, m^2
t_delay=0.04;                  %  delay time, seconds
P_FBV=0.3*P_atm;               %  predominance pressure of FBV, Pa

%  Relay valve parameters
m_rv=0.1;                      %  piston mass of RV, kg
b_rv=12;                       %  viscous friction coefficient of RV, N-s/m
k_rv=1320;                     %  return spring pre-load of RV, N
F_PL_rv=21.32;                 %  return spring pre-load of RV, N
x0_rv=0;                       %  initial position of RV piston, m
x_max_rv=3.5e-3;               %  max displacement of RV piston, m
A_rv=0.0056;                   %  piston area of RV, m^2
Av_rv=28e-6;                   %  orifice area of RV, m^2
P0_rv = 0;                     %  initial pressure in RV, Pa
Pth_rv=6.5*P_atm;              %  threshold pressure of RV (equal to P_st), Pa
```

```
%  Pipeline parameters
d8=0.006;                       %  inner pipe diameter-8x1 polyamide/steel tube, m
d10=0.008;                      %  inner pipe diameter-10x1 polyamide/steel tube, m
d12=0.009;                      %  inner pipe diameter-12x1.5 polyamide/steel tube, m
d1_2=0.0125;                    %  inner pipe diameter-1/2" brake hose, m
L8 = 13.183;                    %  total pipe length-8x1 polyamide/steel tube, m
L10 = 5.436;                    %  total pipe length-10x1 polyamide/steel tube, m
L12 = 11.831;                   %  total pipe length-12x1.5 polyamide/steel tube, m
L1_2 = 1.810;                   %  total pipe length-1/2" brake hose, m

t_sim=2;                        %  total simulation time, seconds

%  run Simulink model
sim pneumatic_air_brake

%  plots
figure(1)
plot(t,x_f*1000,'c','LineWidth',1.6)
hold on
plot(t,x_r*1000,'b','LineWidth',1.6)
hold on
plot(t,x_rv*1000,'r','LineWidth',1.6)
grid
axis([0 max(t) 0 30 ])
title('Piston/Push-rod position vs. time')
xlabel('Time, s')
ylabel('Piston/Push-rod position, x(t), mm')
legend('x_f(t)','x_r(t)','x_r_v(t)','location','southoutside','orientation','horizont
al')

figure(2)
plot(t,P_f/P_atm,'c','LineWidth',1.6)
hold on
plot(t,P_r/P_atm,'b','LineWidth',1.6)
hold on
plot(t,P_rv/P_atm,'r','LineWidth',1.6)
grid
title('Chamber pressure vs. time')
xlabel('Time, s')
ylabel('Chamber pressure, P(t), bar')
legend('P_f(t)','P_r(t)','P_r_v(t)','location','southoutside','orientation','horizont
al')

figure(3)
plot(t,w_f,'c','LineWidth',1.6)
hold on
plot(t,w_r,'b','LineWidth',1.6)
hold on
plot(t,w_rv,'r','LineWidth',1.6)
grid
title('Mass-flow rate vs. time')
xlabel('Time, s')
ylabel('Mass-flow rate, w(t), kg/s')
legend('w_f(t)','w_r(t)','w_r_v(t)','location','eastoutside')
```

```
%
%   Valve_front.m
%
%   This M-file models the mass-flow rate of air in/out
%   of the front brake chamber.  Assumes flow through the
%   valve is air flow through a sharp-edged orifice.
%
%   Inputs:  u (4x1 vector) = [ P_s_f Av P_f dP_f ]'
%                P_s_f = supply pressure/front, Pa
%                Av = valve orifice area, m^2
%                P_f = brake chamber pressure/front, Pa
%                dP_f = pressure drop in front circuit, Pa
%
%   Output:  w_f = in/out mass-flow rate/front brake chamber, kg/s
%

function w_f = Valve_front(u)

%  pneumatic constants (air)
gamma = 1.4;        % = cp/cv = ratio of specific heats
Cd = 0.7;           %  discharge coefficient
R = 287;            %  gas constant (air), N-m/kg-K
T = 298;            %  temperature, K

%  System inputs
P_s_f = u(1);       %  supply pressure/front, Pa
Av = u(4);          %  valve orifice area, m^2
P_f = u(2);         %  pressure in brake chamber/front, Pa
dP_f = u(3);        %  pressure drop in front circuit, Pa

%  Determine if flow is from supply tank/front (Av > 0), or if flow
%  is equal to 0 (Av < 0))
if Av >= 0
    Pv = (P_s_f-dP_f);
else
    Pv = 0;
end

%  find up/down stream pressure
P_hi = max(P_f,Pv);     %  highest pressure (upstream)
P_lo = min(P_f,Pv);     %  lowest pressure (downstream)

%  critical pressure ratio (for choked flow)
Cr = (2/(gamma+1))^(gamma/(gamma-1));      %  = 0.528 for air

%  Determine whether or not flow is choked (sonic at throat)
PR = P_lo/P_hi;       %  pressure ratio downstream/upstream of orifice

%  mass-flow rate equations for compressible flow, kg/s
if PR > Cr
    %  flow is not choked
    w_valve_f = sign(Pv-P_f)*Cd*Av*P_hi*sqrt( ((2*gamma/(gamma-1))/(R*T))*(
PR^(2/gamma) - PR^((gamma+1)/gamma) ) );
else
    %  flow is choked (Mach=1 at throat)
    w_valve_f = sign(Pv-P_f)*Cd*Av*P_hi*sqrt(
(gamma/(R*T))*Cr^((gamma+1)/gamma) );
end

w_f=w_valve_f/4;
```

```
%
%   Valve_rear.m
%
%   This M-file models the mass-flow rate of air in/out
%   of the relay valve.  Assumes flow through the
%   valve is air flow through a sharp-edged orifice.
%
%   Inputs:  u (4x1 vector) = [ P_s_r Av P_rv dP_r ]'
%                P_s_r = supply pressure/rear, Pa
%                Av = valve orifice area, m^2
%                P_rv = relay valve pressure, Pa
%                dP_r = pressure drop in rear circuit, Pa
%
%   Output:  w_r = in/out mass-flow rate/relay valve, kg/s
%

function w_r = Valve_rear(u)

%  pneumatic constants (air)
gamma = 1.4;        % = cp/cv = ratio of specific heats
Cd = 0.7;           %  discharge coefficient
R = 287;            %  gas constant (air), N-m/kg-K
T = 298;            %  temperature, K

%  System inputs
P_s_r = u(2);       %  supply pressure/rear, Pa
Av = u(1);          %  valve displacment, m
P_rv = u(3);        %  pressure in relay valve, Pa
dP_r = u(4);        %  pressure drop in rear circuit, Pa

%  Determine if flow is from supply tank (Av > 0), or if flow
%  is equal to 0 (Av < 0)
if Av >= 0
    Pv = P_s_r-dP_r;
else
    Pv = 0;
end

%  find up/down stream pressure
P_hi = max(P_rv,Pv);     %  highest pressure (upstream)
P_lo = min(P_rv,Pv);     %  lowest pressure (downstream)

%  critical pressure ratio (for choked flow)
Cr = (2/(gamma+1))^(gamma/(gamma-1));      %  = 0.528 for air

%  Determine whether or not flow is choked (sonic at throat)
PR = P_lo/P_hi;       %  pressure ratio downstream/upstream of orifice

%  mass-flow rate equations for compressible flow, kg/s
if PR > Cr
    %  flow is not choked
    w_r = sign(Pv-P_rv)*Cd*Av*P_hi*sqrt( ((2*gamma/(gamma-1))/(R*T))*(
PR^(2/gamma) - PR^((gamma+1)/gamma) ) );
else
    %  flow is choked (Mach=1 at throat)
    w_r = sign(Pv-P_rv)*Cd*Av*P_hi*sqrt( (gamma/(R*T))*Cr^((gamma+1)/gamma)
);
end
```

```
%
%   Valve_rv.m
%
%   This M-file models the mass-flow rate of air in/out
%   of the rear brake chamber.  Assumes flow through the
%   valve is air flow through a sharp-edged orifice.
%
%   Inputs:  u (4x1 vector) = [ P_s_r Av_rv P_r dP_r ]'
%                P_s_r = supply pressure/rear, Pa
%                Av_rv = relay valve orifice area, m^2
%                P_r = brake chamber pressure/rear, Pa
%                dP_r = pressure drop in rear circuit, Pa
%
%   Output:  w_rv = in/out mass-flow rate/rear brake chamber, kg/s
%

function w_rv = Valve_rv(u)

%  pneumatic constants (air)
gamma = 1.4;         % = cp/cv = ratio of specific heats
Cd = 0.7;            %  discharge coefficient
R = 287;             %  gas constant (air), N-m/kg-K
T = 298;             %  temperature, K

%  System inputs
P_s_r = u(2);          %  supply pressure/rear, Pa
Av_rv = u(1);          %  valve orifice area, m^2
P_r   = u(3);          %  pressure in brake chamber/rear, Pa
dP_r  = u(4);          %  pressure drop in rear circuit, Pa

%  Determine if flow is from supply tank/rear (Av_rv > 0), or if flow
%  is equal to 0 (Av_rv < 0)
if Av_rv >= 0
    Pv = (P_s_r-dP_r);
else
    Pv = 0;
end

%  find up/down stream pressure
P_hi = max(P_r,Pv);     %  highest pressure (upstream)
P_lo = min(P_r,Pv);     %  lowest pressure (downstream)

%  critical pressure ratio (for choked flow)
Cr = (2/(gamma+1))^(gamma/(gamma-1));      %  = 0.528 for air

%  Determine whether or not flow is choked (sonic at throat)
PR = P_lo/P_hi;       %  pressure ratio downstream/upstream of orifice

%  mass-flow rate equations for compressible flow, kg/s
if PR > Cr
    %  flow is not choked
    w_valve_rv = sign(Pv-P_r)*Cd*Av_rv*P_hi*sqrt( ((2*gamma/(gamma-
1))/(R*T))*( PR^(2/gamma) - PR^((gamma+1)/gamma) ) );
else
    %  flow is choked (Mach=1 at throat)
    w_valve_rv = sign(Pv-P_r)*Cd*Av_rv*P_hi*sqrt(
(gamma/(R*T))*Cr^((gamma+1)/gamma) );
end

w_rv=w_valve_rv/4;
```

```
%
%  M-file for computing the pressure-rate (P-dot_front)
%  for the air-brake chamber/front
%
%   Input:  u (4x1 vector) = [ w_f x_f xdot_f P_f ]'
%               w_f = mass flow-rate in/out chamber (kg/s)
%               x_f = diaphragm-piston position, m
%               xdot_f = diaphragm-piston velocity, m/s
%               P_f = brake chamber pressure/front, Pa
%
%   Output: dPdt_f = dP/dt, Pa/s
%

function dPdt_f = Pdot_front(u)

%  brake chamber parameters/front
Ab_f = 0.00774;       %  area of diaphragm-front brake chamber, m^2
V0_f = 0.12e-3;       %  volume of front brake chamber when x=0, m^3

R = 287;              %  gas constant (air), N-m/kg-K
n = 1;                %  polytropic expansion index
T = 298;              %  air temperature, K

%  system inputs
w_f    = u(1);        %  in/out mass-flow rate of air(+ or -), kg/s
x_f    = u(2);        %  diaphragm-piston position, m
xdot_f = u(3);        %  diaphragm-piston velocity, m/s
P_f    = u(4);        %  pressure of brake chamber, Pa

%  compute chamber volume/front and dV/dt
V_f = V0_f + Ab_f*x_f;        %  volume of brake chamber, m^3
Vdot_f = Ab_f*xdot_f;         %  time-rate of volume, m^3/s

%  pressure-rate for brake chamber/front, Pa/s
dPdt_f = ((n*R*T)/V_f)*(w_f - P_f*Vdot_f/(R*T));
```

```
%
%  M-file for computing the pressure-rate (P-dot_rear)
%  for the air-brake chamber/rear
%
%   Input:  u (4x1 vector) = [ w_r x_r xdot_r P_r ]'
%               w_r = mass flow-rate in/out chamber (kg/s)
%               x_r = diaphragm-piston position, m
%               xdot_r = diaphragm-piston velocity, m/s
%               P_r = brake chamber pressure/rear, Pa
%
%   Output: dPdt_r = dP/dt, Pa/s
%

function dPdt_r = Pdot_rear(u)

%  brake chamber parameters/rear
Ab_r = 0.00774;       %  area of diaphragm-rear brake chamber, m^2
V0_r = 0.12e-3;       %  volume of rear brake chamber when x=0, m^3

R = 287;              %  gas constant (air), N-m/kg-K
n = 1;                %  polytropic expansion index
T = 298;              %  air temperature, K

%  system inputs
w_r    = u(1);        %  in/out mass-flow rate of air(+ or -), kg/s
x_r    = u(2);        %  diaphragm-piston position, m
xdot_r = u(3);        %  diaphragm-piston velocity, m/s
P_r    = u(4);        %  pressure of brake chamber, Pa

%  compute chamber volume/rear and dV/dt
V_r = V0_r + Ab_r*x_r;        %  volume of brake chamber, m^3
Vdot_r = Ab_r*xdot_r;         %  time-rate of volume, m^3/s

%  pressure-rate for brake chamber/rear, Pa/s
dPdt_r = ((n*R*T)/V_r)*(w_r - P_r*Vdot_r/(R*T));
```

```
%
%  M-file for computing the pressure-rate (P-dot_rv)
%  for the relay valve
%
%   Input:  u (4x1 vector) = [ w_r x_rv xdot_rv P_rv ]'
%               w_r = mass flow-rate in/out relay valve (kg/s)
%               x_rv = diaphragm-piston position, m
%               xdot_rv = diaphragm-piston velocity, m/s
%               P_rv = relay valve pressure, Pa
%
%   Output: dPdt_rv = dP/dt, Pa/s
%

function dPdt_rv = Pdot_rv(u)

%  relay valve parameters
A_rv = 0.0056;      %  area of diaphragm-relay valve, m^2

V0_rv = 0;          %  volume of relay valve when x=0, m^3
d_cl = 0.006;       %  inner pipe diameter-8x1 tube btw. FBV and RV, m
L_cl = 9.666;       %  pipe length-8x1 tube btw. FBV and RV, m

R = 287;            %  gas constant (air), N-m/kg-K
n = 1;              %  polytropic expansion index
T = 298;            %  air temperature, K

%  system inputs
w_r    = u(1);      %  in/out mass-flow rate of air(+ or -), kg/s
x_rv    = u(2);     %  diaphragm-piston position, m
xdot_rv = u(3);     %  diaphragm-piston velocity, m/s
P_rv    = u(4);     %  pressure of relay valve, Pa

%  compute total dead volume
V_cl = (pi()*d_cl^2/4)*L_cl;
V0 = V0_rv+V_cl;

%  compute relay valve volume and dV/dt
V_rv = V0 + A_rv*x_rv;     %  volume of relay valve, m^3
Vdot_rv = A_rv*xdot_rv;    %  time-rate of volume, m^3/s

%  pressure-rate for relay valve, Pa/s
dPdt_rv = ((n*R*T)/V_rv)*(w_r - P_rv*Vdot_rv/(R*T));
```

CURRICULUM VITAE

Name Surname **: İbrahim Can GÜLERYÜZ**

Place and Date of Birth **: Bornova, 02.05.1989**

E-Mail **: can.guleryuz@hotmail.com**

EDUCATION **:**

- **B.Sc.** **:** 2012, Dokuz Eylül University, Faculty of Engineering. Mechanical Engineering Department

PROFESSIONAL EXPERIENCE AND REWARDS:

- April 2017-…: CMS Wheels, R&D Center, Project Engineer.
- January 2016-April 2017: BMC, R&D Center, Brake System Engineer.
- February 2015-January 2016: Ege Fren, R&D Center, R&D Engineer.
- August 2012-September 2014: Eltas Transformers, Project and R&D Department, Mechanical Engineer.

OTHER PUBLICATIONS, PRESENTATIONS AND PATENTS:

- **Karadeniz Z. H., Guleryuz I. C.,** Investigation of cross-flow wind turbine performance, 2nd Wind Symposium, Izmir, 2015 *(Original: Çapraz akışlı rüzgar türbini başarımının incelenmesi)*